SP-1212

The Global Ozone Monitoring Experiment

GOME

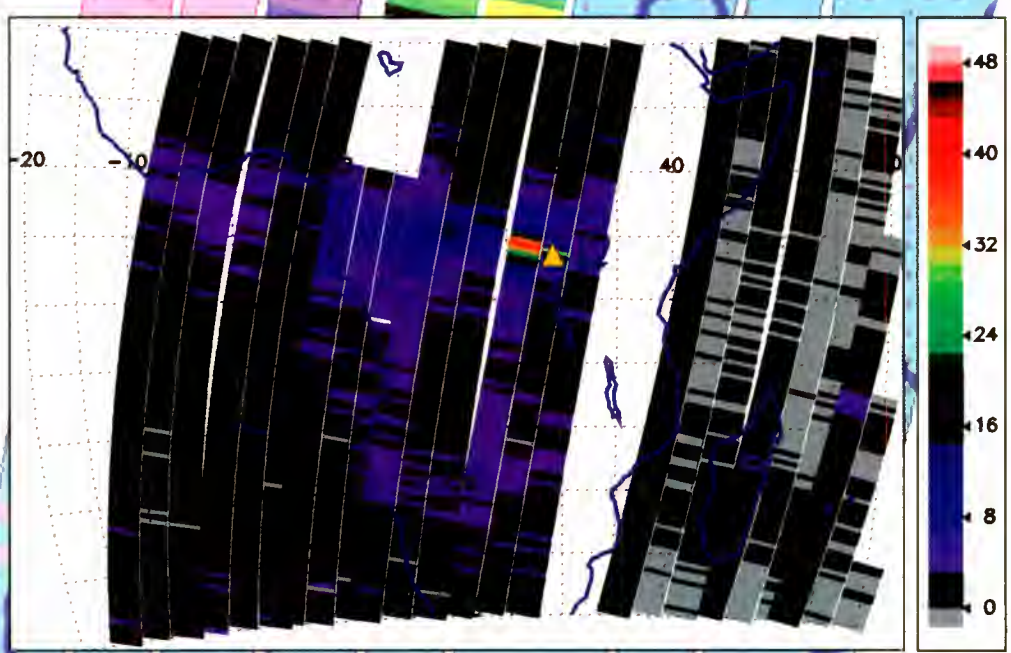

Scientific Achievements of GOME-1 and Expectations for GOME-2

European Space Agency
Agence spatiale européenne

SP-1212
June 1997

The Global Ozone Monitoring Experiment

Scientific Achievements of GOME-1 and Expectations for GOME-2

A. Hahne

ESA Earth-Observation Projects Department

European Space Agency
Agence spatiale européenne

Cover picture: SO_2 plume from the Nyamuragira volcanic eruption (see page 25)

Published by: ESA Publications Division
ESTEC
PO Box 299
2200 AG Noordwijk
The Netherlands

Editor: Bruce. Battrick
Layout: Isabel Kenny
Cover design: Carel Haakman

Price: 50 DFL

ISBN 92-9092-447-0

Contents

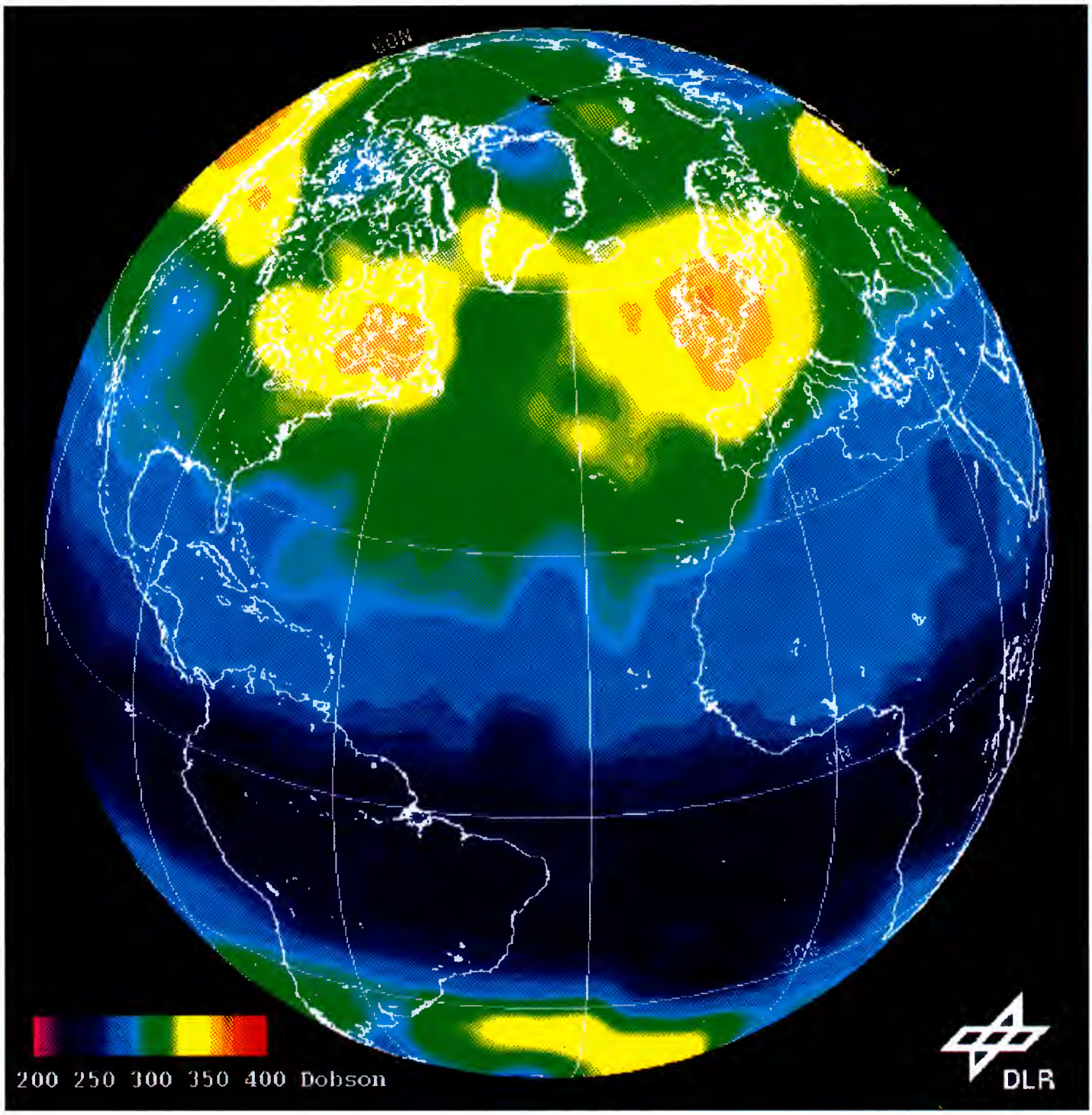

First Operational GOME-1 Total Column Ozone Map for the period 5 - 7 July 1996

1. Introduction

1.1 Scope of the Document

The initial GOME instrument, referred to here as 'GOME-1', was launched onboard ESA's ERS-2 remote-sensing satellite on 21 April 1995. GOME is the only new instrument on ERS-2 compared with ERS-1 and was developed in the same time frame in which the satellite and its payload were constructed based on the ERS-1 design. One constraint imposed upon the GOME instrument was that its resource demands had to be compatible with the available system margins established by the ERS-1 mission.

Another programmatic constraint for GOME was that no financial allocations were made within the ESA Earth-Observation Programme for the processing of the data coming from the instrument. Instead, these costs were supposed to be covered by national undertakings of the ESA Member States. As a result, only the basic processor generating radiance/irradiance and total ozone column products is operational to date.

In late 1996, the ESA Programme Board for Earth Observation and Eumetsat's Council decided to procure an enhanced version of the GOME instrument, termed 'GOME-2', to be flown on the METOP series of operational meteorological satellites being developed jointly by ESA and Eumetsat. On the basis of the 'lessons learnt' from the GOME-1 operations and data evaluation, and given that the resource restrictions for METOP are not quite as stringent as for ERS-2, some modifications to the instrument's design and performance parameters are envisaged which will strengthen its scientific and operational capabilities.

This document reports on what can be expected from such an improved instrument. In order to underpin the case, the achievements of the existing instrument, GOME-1, in terms of instrument performance, routinely generated data products, and scientific results achieved so far are first summarised, before extrapolating to the expected performances and capabilities of the enhanced version GOME-2 being built for METOP.

1.2 Background Information: GOME-1

The scientific rationale underlying GOME-1's development is reported in ESA Special Publication SP-1151, titled 'The Global Ozone Monitoring Experiment: The Interim Science Report'. In addition to describing the general mission rationale, it justifies key instrument and calibration requirements, outlines the basics of the proposed retrieval algorithm to be applied to the data, and provides background information on the reference spectra of the species to be retrieved and on the associated signal-to-noise and sensitivity studies.

The design, building, testing and calibration of the instrument itself (Fig. 1.1) is exhaustively described in ESA Special Publication SP-1182, titled 'GOME Users Manual'. This manual also provides information on the contents and formats of the data products (as then defined) generated from the instrument's science data stream. The most recent version of this product specification can be obtained from the German Aerospace Research Establishment DLR (see Section 3).

After the launch and initial technical commissioning of GOME-1 aboard ERS-2, the data products underwent a thorough validation by some more than 20 scientific groups selected by means of an 'Announcement of Opportunity'. The results of this validation campaign are reported in 'GOME Geophysical Validation Campaign, Final Results',

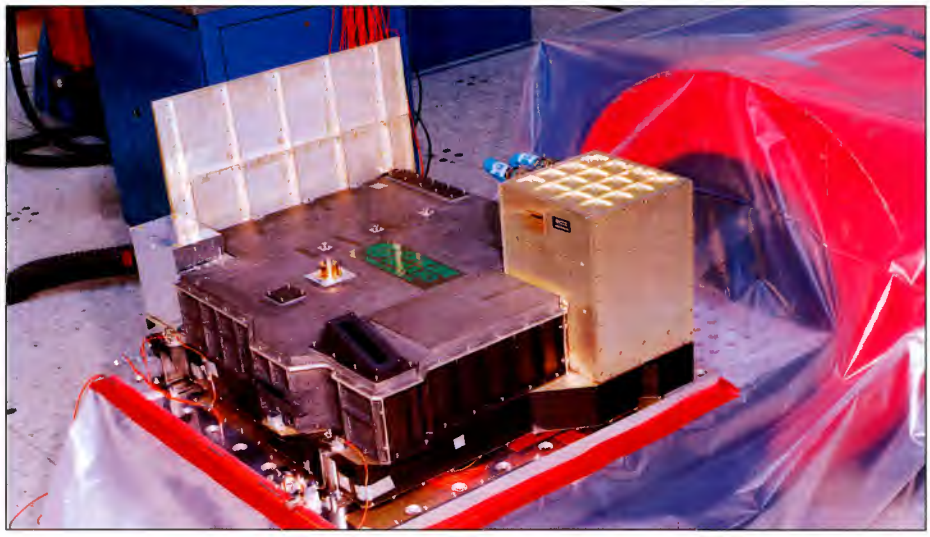

Figure 1.1. The GOME-1 instrument during environmental (vibration) testing

ESA Workshop Proceedings WPP-108. Most of the resulting recommendations for modifications to key calibration data, processor parameters, and operational procedures have been implemented in the meantime. Despite the reference to 'Final Results' in the title of WPP-108, validation activities are still continuing. At the time of writing, the Third ERS Scientific Symposium has just been held in Florence, Italy (March 1997), and the Proceedings are presently in print, as ESA Special Publication SP-394. Many of the results reported here are gleaned from the presentations, posters and demonstrations given at that Symposium.

1.3 GOME-2: Technical Features

GOME-2 will provide improved performances in several areas compared with GOME-1, including the following:

Polarisation measurements
The present polarisation measurement scheme uses the polarisation sensitivity of the instrument as measured on the ground prior to launch, and the data from three onboard broadband polarisation detectors (grossly matching the spectral coverage of channels 2, 3 and 4) in the plane parallel to the slit to correct the radiance values for polarisation effects. Although this scheme works satisfactorily, there is the desire to enhance these measurements by:

- measuring the degree of polarisation of the incoming light in two orthogonal planes, in order to have an additional source of information for cloud type distinction and aerosol retrieval
- improving the wavelength resolution beyond the three broadband channels used so far. A target value that looks feasible from the implementation point of view is to have 10 channels per polarisation direction for the wavelength range from 300 to 800 nm.

Swath width and scan profile
Whilst with GOME-1 the maximum swath is limited to ±31 degrees, corresponding to 960 km on the ground from ERS-2's orbit (altitude 780 km), GOME-2 will have the

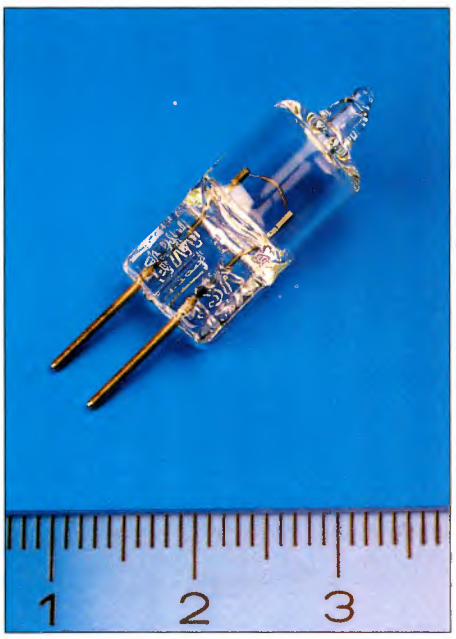

Figure 1.2. White-light source (quartz tungsten halogen lamp) for GOME-2 with a centimetre ruler

ability to scan a swath of 1920 km from the METOP orbit of (nominally) 824 km. The impact of such a larger swath on retrieval accuracies, e.g. for cloud top height/cloud type or for ozone profile retrieval, still needs to be assessed in detail.

Another modification concerns the scan-speed profile, which can be adjusted so that the ground scene size variation, due to the oblique viewing and the Earth's curvature, will be minimised in the across-track direction.

Relative radiometric calibration

Driver for implementing means for a relative radiometric calibration tool is the etalon which is present on the cooled Reticon detectors, due to the protective SiO_2 layer and due to freezing water vapour. Although, as expected, this etalon stabilises in the vacuum of space, it is irritating during the ground calibration and for the transfer of key calibration data between the on-ground measurements and the initial in-orbit situation. GOME-2 will therefore include a quartz/tungsten halogen lamp (Fig. 1.2) with a filament temperature of about 2800 K, similar to those used for the same purpose in ground-based DOAS instruments.

Integration times and spatial sampling

Rather than using the default 1.5 sec integration time on the Reticon detectors, which corresponds to a ground-scene size of 320x40 km^2 at 960 km swath, the GOME-2 sampling will be at 0.1875 sec corresponding to 40x40 km^2 for the same swath. This is achieved by removing diaphragms presently used to avoid saturation in channels 2 to 4. The resulting eight-fold increase in spatial resolution boosts the data rate to be transmitted by approximately the same factor.

In the ultraviolet channel 1, presently operated on GOME-1 with a default integration time of 12 sec, ground-scene size can be reduced by a faster readout (e.g. 1.5 sec), and recovery of signal-to-noise ratio by co-adding, on the ground, 10 pixels in the spectral domain. This is made feasible by the fact that the Hartley band of ozone is not very structured in the region with the lowest signal.

Other modifications

Other modifications to GOME-2 are mainly driven by system factors such as orbit, satellite accommodation differences between ERS-2 and METOP, and some minor 'lessons learnt'. None of them are expected to have any impact on the instrument's general performance and scientific capabilities.

2. GOME Instrument Performance

2.1 General

The performance of the instrument proper as described in this section does, of course, have an impact on the level-1 data product reported in Section 3. However, there are features such as lifetime, radiation effects, etc. which do not necessarily show up in the data products, and this section will report on some essential instrument performance and calibration features. Some of the instrument-related problems are corrected for in the ground processing to level 1 and will (again) be addressed there.

Generally speaking, the GOME instrument has demonstrated excellent performance, and most observed degradations are as expected and have been accounted for by devising the on-board calibration tools accordingly.

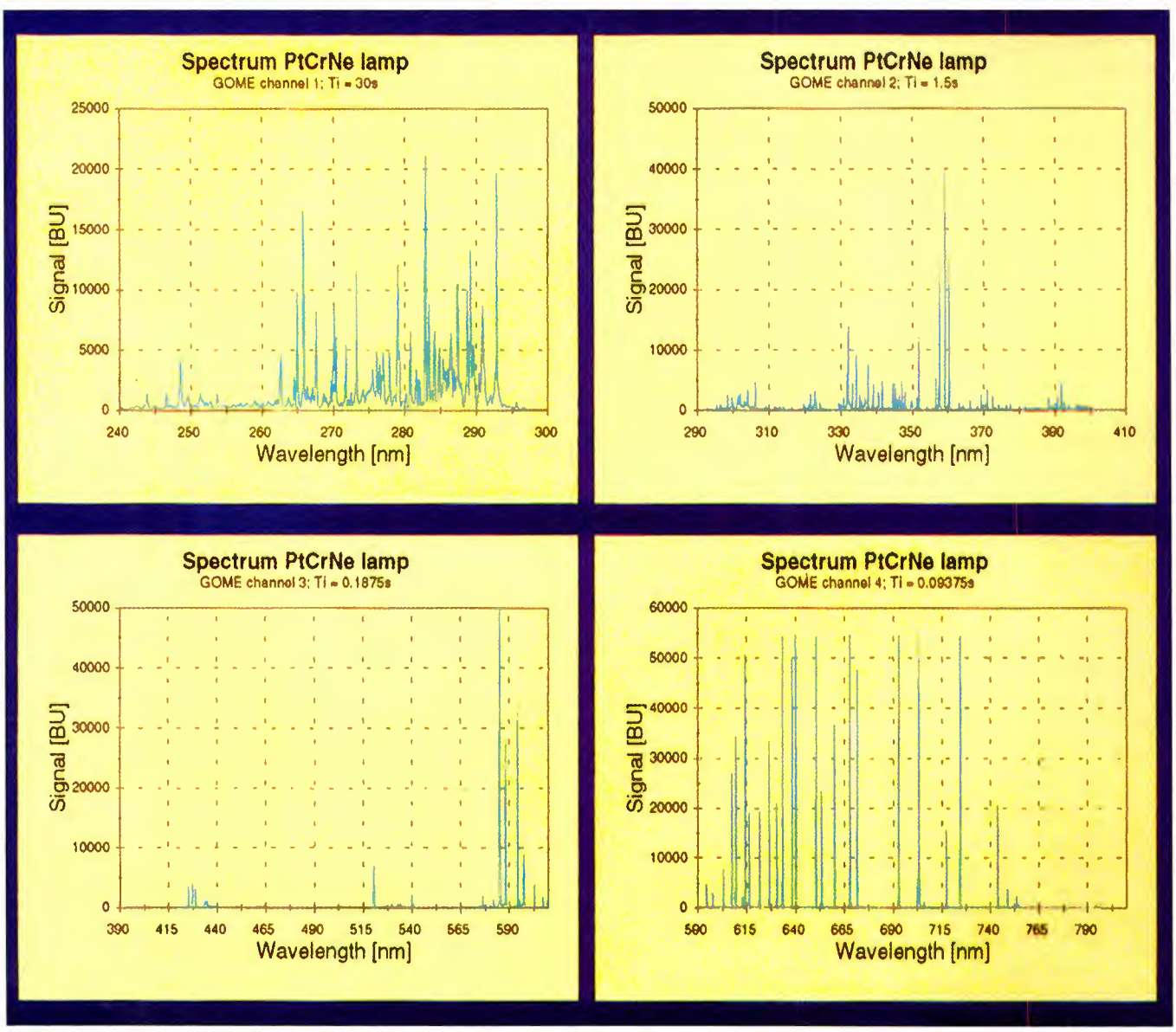

Figure 2.1. Wavelength calibration lamp spectrum as recorded by GOME

2.2 Wavelength Registration and Stability

The primary means for determining the wavelengths impinging on the individual detector pixels are the sharp emission lines from the onboard wavelength calibration lamp (Fig. 2.1). A high-resolution spectrum of this lamp recorded prior to launch is used to select suitable lines for the calibration. With this selection and a suitable algorithm to determine the line centres and to interpolate for the regions in between lines, the wavelength determination accuracy is generally of the order of 1/50th of a detector pixel.

There are some problematic regions, particularly near the channel boundaries, where there are no or only weak or distorted lines, degrading the wavelength determination accuracy in these regions. Revisiting the line selection, the order of polynomial fitting for the entire channel and a revision of the slit function coefficients have been initiated and are expected to provide some improvements. Significant improvements have been demonstrated with techniques using the Fraunhofer structure in irradiance and radiance spectra[1], but the algorithms are not (yet) being used operationally.

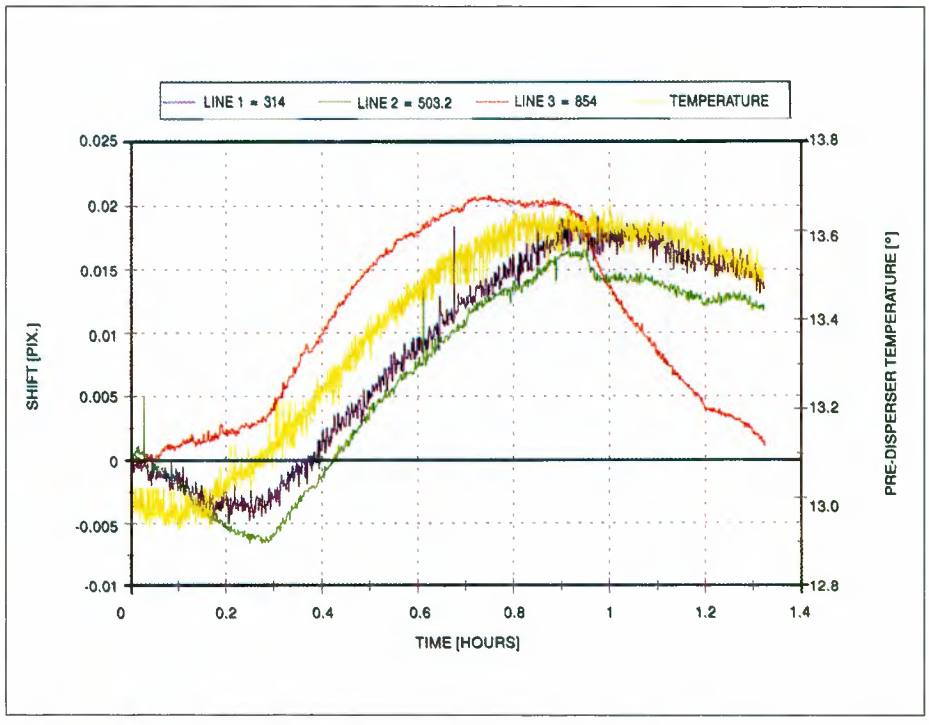

Figure 2.2 Wavelength stability over one orbit

The stability of the wavelength registration mapped over one orbit is shown in Figure 2.2. To a first approximation, it is a function of the pre-disperser prism temperature, which is shown in yellow in the plot. The wavelength drift as a function of pre-disperser temperature is recorded once a month during the regular calibration campaign, and used in the ground processing for wavelength determination for the radiance spectra[2].

2.3 Radiometric Performance and Stability

2.3.1 Ground calibration

The activities performed during the ground calibration of the instrument are reported in detail in chapter 6 of Reference 3. Note in particular the cross-reference between the standards used for the GOME-1 calibration and the NASA integrating sphere used for the calibration of the TOMS and SBUV instruments, which show excellent agreement within the absolute accuracy limits of the two standards (Fig. 2.3).

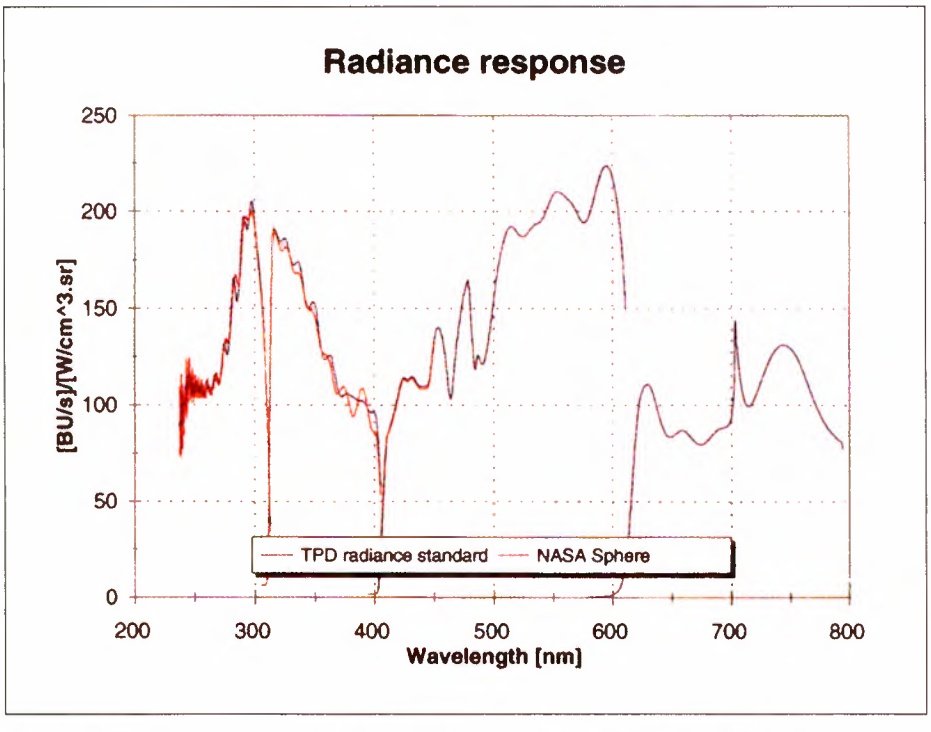

Figure 2.3. Result of cross-calibration between TPD FEL lamp and NASA integrating sphere

2.3.2 Noise performance

The rms readout noise has been measured to be 1700 electrons (e^-) equivalent to 2 Binary Units (BU). With the detectors being cooled to -38 deg C, and a demonstrated thermal stability in all four channels of about 0.2 K all around the orbit, the leakage current is negligible for the shortest readouts. For longer integration times, the leakage current is measured during the dark part of the orbit and subtracted in the ground processing.

With a full dynamic range of about 60000 BU (exact value depends on the capacitance of each individual detector), the signal to noise ratio achieved at an average albedo of 0.3 is in the order of several thousand in most spectral regions. Exceptions are the overlap regions, where the light is successively split between two channels and hence the signal level decreases accordingly, and the lower ends of both channels 1 and 2. One problem which initially affected channel 1 was some observed cross-talk between the power supply lines of the Peltier element used for detector cooling and the analogue readout. However, with knowledge of the power switching of the Peltier control loop, the problem could be reduced by a factor of 10 and is now in the order of 1-2 BUs (see Ref. 36).

Stray light had been thoroughly characterised during the ground characterisation, both in the form of uniform background stray light and as ghost images caused by back reflections between the various optical surfaces. Stray light is measured on a number of non-illuminated detector pixels in channels 1 and 2 (the most critical channels in this respect), and a stray-light correction 'option' based on the on-ground calibration is provided in the level-1 data set. For all practical purposes, however, one can neglect stray light in most parts of the recorded spectrum.

2.3.3 Gain stability

The only area of concern in this respect is the possibility of permanent damage to individual detector pixels from hard cosmic radiation. To monitor this, each channel objective carries a Light Emitting Diode (LED) used to monitor the relative health of the detectors on a regular basis. No significant change has been observed so far, after two years in orbit.

2.3.4 Instrument stability

The space vacuum, radiation environment, exposure to solar radiation, thermal cycling, etc. all have an impact on the long-term stability of the instrument. To cope with this, various means of calibration and monitors are implemented to keep track of these changes and to be able to deal with them during the ground processing. The following effects have been observed:

Coating offgassing: Once in vacuum, the anti-reflection coatings on the numerous optical surfaces undergo an offgassing/water desorption process, which has an impact on the radiometric throughput of the instrument. This is a rather rapid process and stabilises after a few days in orbit, because the coatings involved are rather thin. The effect has been confirmed by air/vacuum comparisons made within the GOBELIN measurements with the GOME breadboard model[4]. The quantitative correction used the wavelength calibration lamp line ratios, normalised for the total output pre- and post launch, to account for this effect.

Figure 2.4 Dichroic features of the channel 3/4 beam splitter

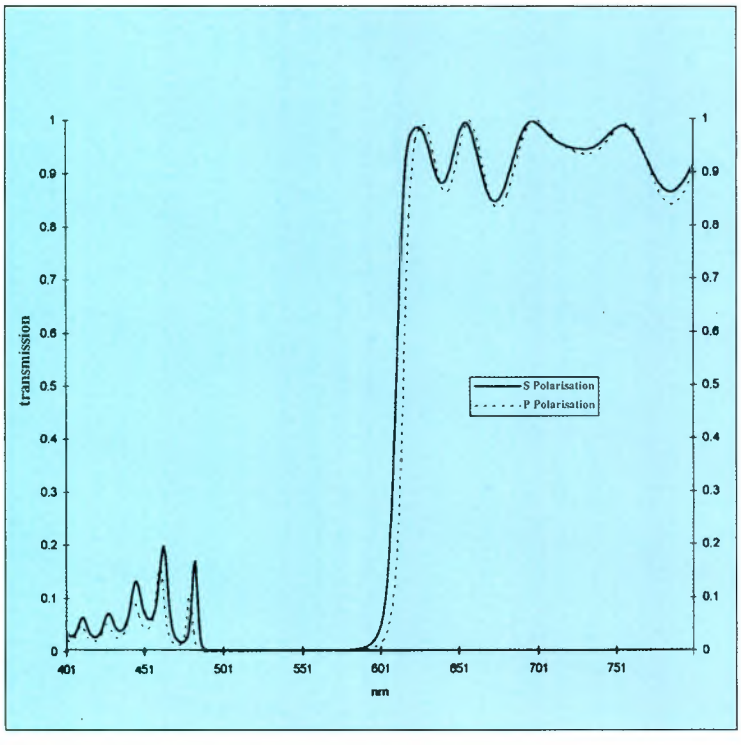

Dichroic shift: The dichroic beam splitter, used to separate channels 3 and 4, is a steep cut-off filter with many layers. This filter, once in vacuum, also releases volatiles and hence changes optical properties. Because of the multi-layer design, this release is controlled by diffusion and occurs over an extended period. The result is not only a shift in the cut-off wavelength, but it also affects some modulation features in the transmission efficiency, which also change accordingly (Fig. 2.4). These features can then be used to correct for the effect: Using the pre-flight pattern as a reference, the amplitude and phase can be determined in a 'quasi DOAS' procedure with 'shift and squeeze', and then stored in a dynamic database updated at regular intervals.

UV transmission degradation: From time series of solar irradiance measurements and comparisons with SOLSTICE data[5,6], one can derive a reduction in optical transmission in the UV region of about 12% per year at 240 nm[6]. Such a degradation is not unexpected and is the reason why solar calibrations

are performed. The important question, however, is whether this degradation is in the optical path common to the irradiance and radiance measurements, or whether it is specific to the irradiance path with the diffuser as most prominent optical element.

The diffuser can be monitored by channelling the light from the wavelength calibration lamp via the diffuser, and ratioing it with the direct lamp view. Assuming that the lamp's output is stable over this relatively short period, time series of this ratio can be used for monitoring the diffuser reflectivity.

Within the signal-to-noise limits of the method, no diffuser degradation could be detected[8]. This means that the degradation is common to both the irradiance and radiance paths, and hence does not affect the retrieval of ozone and other trace gases, which use the 'Sun-normalised radiance' (I/F) as a starting point.

An independent confirmation of this conclusion is provided by the evaluation of Moon observations[7], which use only the 'radiance' part of the optical train.

2.3.5 Etalon effect

This is the only effect for which a real remedy has not yet been found. It is caused by water vapour freezing out on the cooled detectors, and hence forming a time-varying layer in which an etalon structure builds up. This leads to a modulation of the radiometric response, with an amplitude of up to several percent.

As expected, the rate of change of this ice layer stabilised within the instrument commissioning phase such that, between the daily Sun calibrations, the rate of change is negligible. Consequently, the remaining effect that the etalon has is in:

- impacting on the initial 'key data set' from the ground calibration
- comparisons of absolute irradiance values (and, in principle, radiance as well) over extended periods
- a change in 'starting conditions' after an instrument switch-off; after which a Sun calibration therefore needs to be performed within the next orbit.

2.4 Polarisation

The GOME-1 instrument shows a pronounced variation in polarisation sensitivity as a function of wavelength, which has been characterised pre-launch, including the effects of scanning-mirror position. The only variable is the degree of polarisation of the incoming light in radiance measurements. To account for this, the 'Polarisation Measurement Device' measures in three broadband channels in one polarisation direction. These measurements are complemented by the 'seventh point', which is a theoretically established value for the UV at 300 nm, where meaningful measurements are not possible because of the low photon fluxes and detector efficiencies.

The validity of this approach can be verified for some well-defined geometrical conditions, and has been proved to work sufficiently accurately[9].

2.5 Radiation Effects

Space radiation (cosmic rays, solar protons and electrons) has several effects on the instrument's performance:

Figure 2.5 Radiation spikes in the spectrum

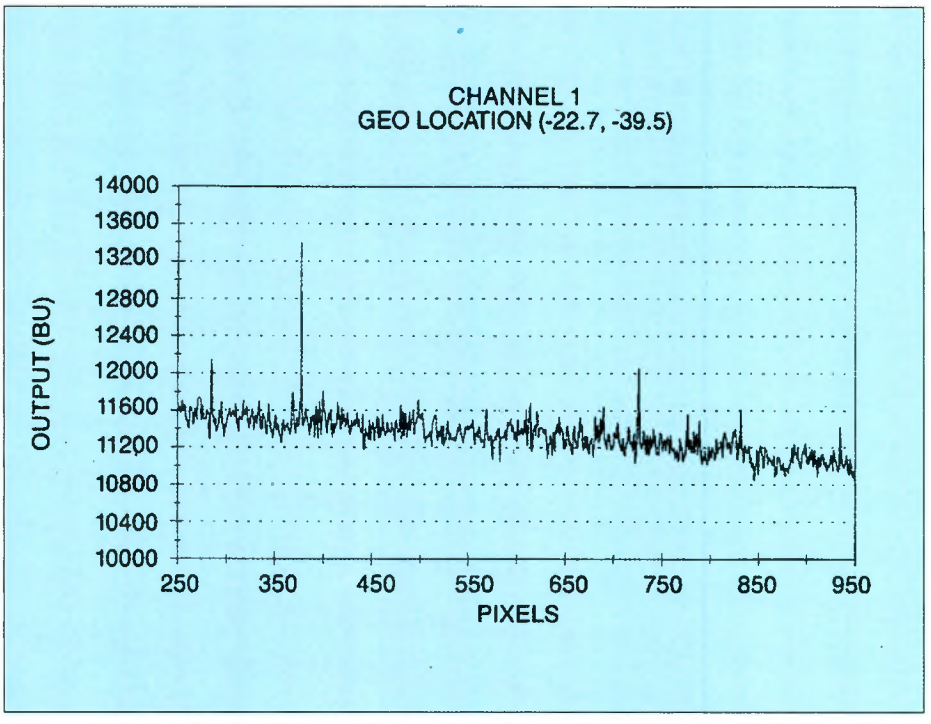

- Spikes in the spectra (Fig. 2.5) by radiation releasing charge in the detector pixels[2]. These spikes are filtered out in the processing.
- Increased noise levels, particularly for measurements in channel 1 with relatively long integration times. For most of the orbit, this is not of real concern, except for dark-current measurements performed in the South Atlantic Anomaly (SAA)[2.10]. Dark-current measurements in the vicinity of the SAA are therefore discarded.
- Accumulated dose effects, which cause radiation damage to the silicon substrate of the detectors (lattice defects). The result is a gradual increase in dark current at a rate of about 15% per year[8].

2.6 Pointing Accuracy and Localisation

Pointing accuracy

Early in the commissioning phase, a pointing evaluation was been performed on the first two Moon calibrations. Because of the instrumentís sideways viewing towards the Moon (between 78 and 86 deg w.r.t. nadir), lunar calibrations are very sensitive to roll-axis errors (the axis about which the scan mirror rotates). The evaluation concluded that the combined satellite and instrument errors about the roll axis are -0.030 ±0.013 degree. (Because the mirror had been used for normal observations in between, the 0.012.deg SDEV is the reproducibility of the mirror positioning plus the satellite's rate error).

Subsequent lunar observations have not been evaluated for this aspect, but the fact that there was never a reported problem in seeing the Moon confirms the stability of the pointing accuracy.

Localisation

Being largely determined by the satellite localisation accuracy, which is well below

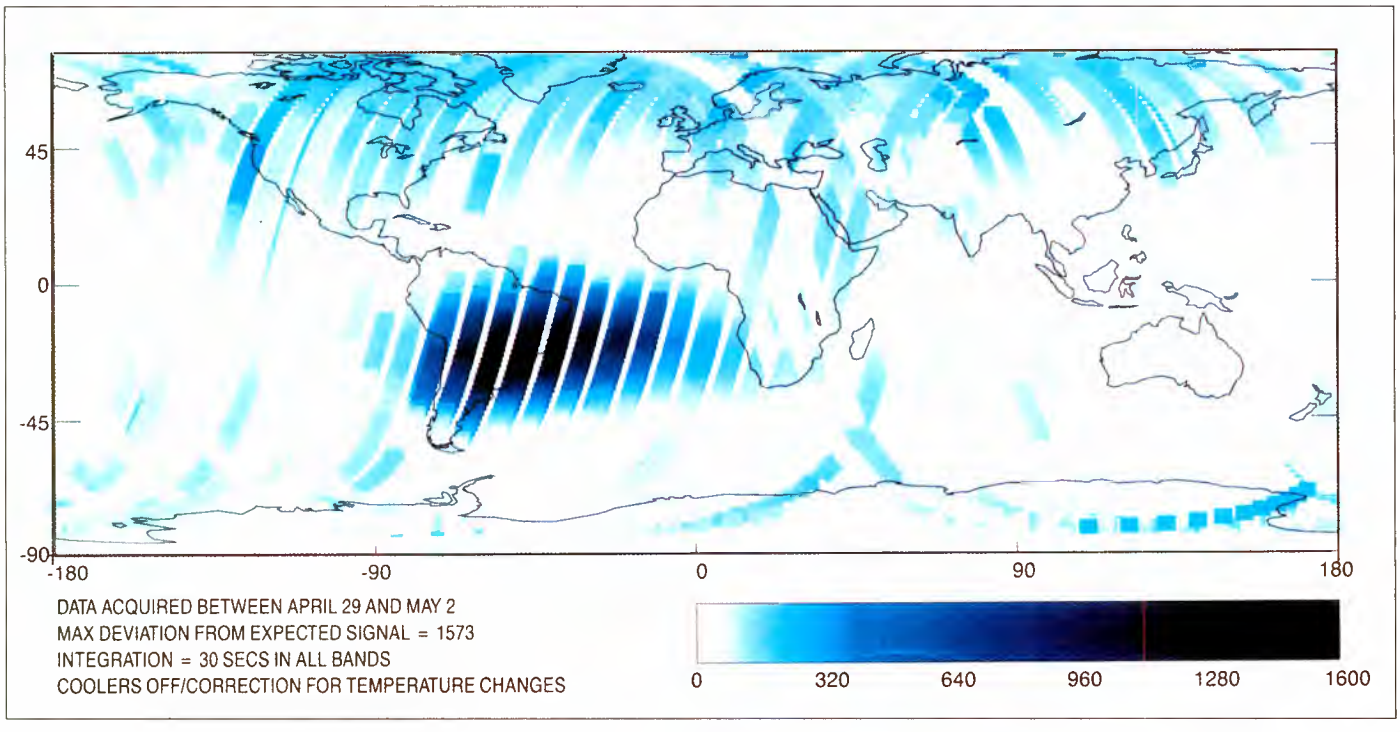

Figure 2.6. Global map of (highest detected) radiation spikes. The dark-blue region outlines the 'South Atlantic Anomaly'

1 km both along and across track, the localisation accuracy for the GOME ground scenes is better than 3 km in the worst case.

2.7 Lifetime

The life-limited items of the GOME instrument are:
- the scanner bearings
- the wavelength calibration lamp.

Scanner bearings
Before finally selecting the bearings presently used in the GOME instrument, bearings of the same type (with the same lubricant) were subjected to accelerated life-testing under representative conditions (vibration, vacuum, pre-loading, temperature). The test was stopped after 60 million cycles, without any noticeable sign of degradation or wear (60 million cycles correspond to approx. 18 years of continuous operation!). Having now (March 97) performed about 6 million cycles in-orbit, there are still no signs of wear or degradation, as can be concluded from statistics of position accuracy and torque telemetry.

Wavelength calibration lamp
The wavelength calibration lamp was also subjected to life-testing prior to its selection. Any degradation manifests itself in a gradual reduction of lamp output. Despite its intensive use in the ground calibration and now about 225 hours in orbit, the lamp's output still shows no significant degradation.

3. GOME-1 Data Products

3.1 The GOME Data Processor (GDP)

The GOME Data Processor (GDP) was developed, and is operated by the German Aerospace Research Organisation (DLR) in Oberpfaffenhofen near Munich, with funding mainly provided by the German Space Agency (DARA). Numerous scientists from the Universities of Bremen and Heidelberg, the Max-Planck-Institute for Chemistry in Mainz, and the Smithsonian Institute in Cambridge (USA) contributed inputs to the processor. The processing of GOME data is embedded into the 'Data Management System' inherited from ERS-1, which is providing the 'overhead functions' in terms of data ingestation and sorting, processing supervision, order handling, product delivery, archiving and cataloguing.

Two levels of product are being generated by the GDP:

Level 1: Radiance/irradiance, consisting of wavelength and radiometrically calibrated, time-stamped and geo-located radiance and irradiance spectra (irradiance is measured once a day)
Level 2: Total ozone column amount, based on 'Differential Absorption Spectroscopy (DOAS)' retrieval. In this product, NO_2 columns and the fractional cloud cover are also reported.

Level-1 products (for ESA Project Scientists) and level-2 products can be ordered via

ESRIN ERS Help Desk, Frascati, Italy
Tel: +39-(6)-94180666
Fax: +39-(6)-94180272
Email: eohelp@esrin.esa.it

The formats of available data products are defined in the Product Specification Document of the GOME Data Processor, ER-PS-DLR-GO-0016, Issue 3C, which can be consulted at:

http://www.dfd.dlr.de/info/AUC/GOME/index.html

whilst the algorithms used are described in:

- GOME Level 0 to 1 Algorithms Descriptions
  ER-TN-DLR-GO-0022, Issue 4A

- GOME level 1 to 2 Algorithms Descriptions
  ER-TN-DLR-GO-0025, Issue 2A

3.2 Level-1 Product: Radiance/Irradiance

3.2.1 Processing steps

In addition to the conversion from binary telemetry to engineering units, the processing involves the following steps:
- radiation-induced-spike removal
- leakage-current correction
- Peltier cross-talk noise correction
- pixel-to-pixel gain correction

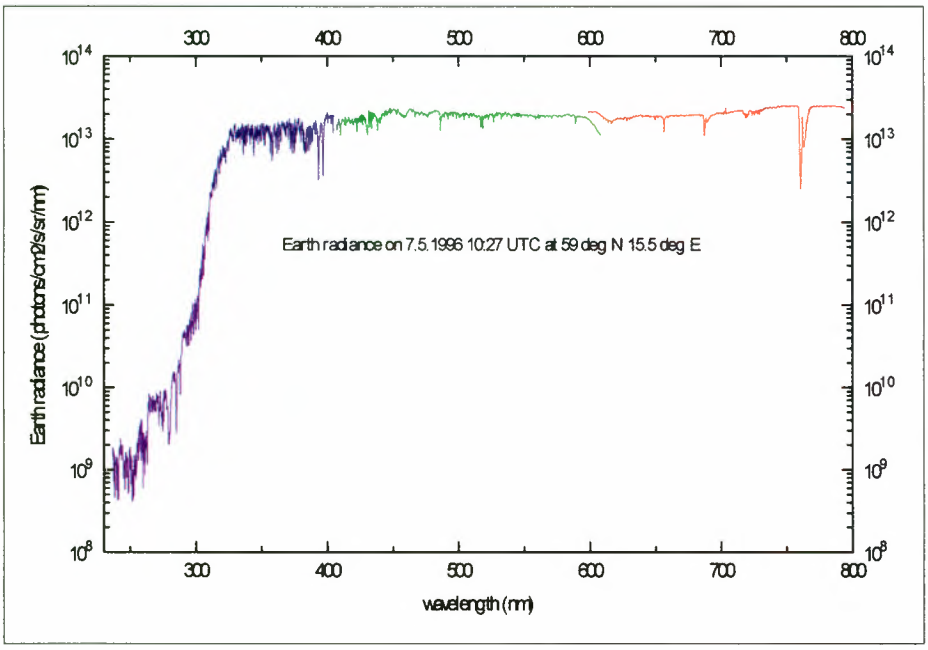

Figure 3.2.1 Earth radiance from 237 to 790 nm measured by GOME-1 on 7 May 1996 at 59°N. All four channels are shown: Channel 1 (violet), Channel 2 (blue), Channel 3 (green) and Channel 4 (red). Overlap region 3/4 is clearly visible

- stray-light correction
- spectral calibration
- radiometric calibration
- polarisation correction
- geolocation computation
- quality flagging and error computation.

Figures 3.2.1 and 3.2.2 show examples of the level-1 product. Figure 3.2.1 shows a complete radiance spectrum for a completed integration time of 12 seconds. Note that intermediate spectra, acquired every 1.5 sec (onboard co-added from four spectra, because of telemetry limitations), are lacking the lowest part of the wavelength range, 240-307 nm.

Figure 3.2.2 shows an irradiance spectrum, acquired once a day, for about 42 sec on average, and reported in every radiance product (one product file comprises spectra from one full orbit).

3.2.2 Validation status

Because of the variability of the atmosphere in time and space, a true validation of the radiance measurements is extremely difficult. A very limited validation has been performed with the visible channels at 555 and 659 nm of the Along-Track Scanning Radiometer (ATSR-2) aboard ERS-2, by co-adding GOME spectra to the ATSR bandpass, and by summing ATSR 1x1 km pixels to the scene size of the GOME measurements[11]. The results agree very well within the quoted radiometric accuracies of the two instruments.

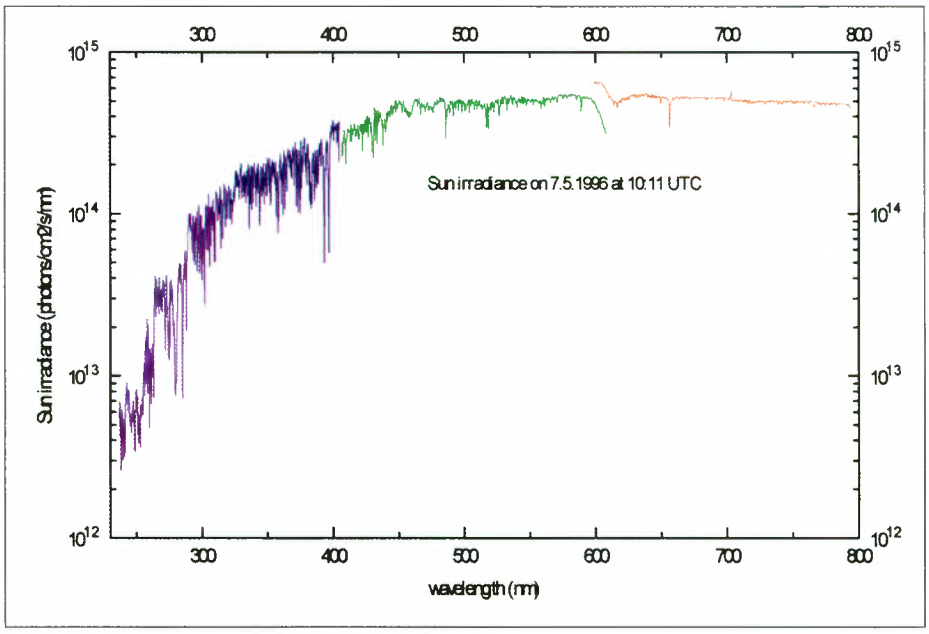

Figure 3.2.2 Sun irradiance from 237 to 790 nm measured by GOME-1 on 7 May 1996. All four channels are shown: Channel 1 (violet), Channel 2 (blue), Channel 3 (green) and Channel 4 (red). Overlap region 3/4 is clearly visible

For the irradiance, comparisons have been performed with the data from SOLSPEC and SSBUV, and are continuing to be performed with SOLSTICE on-board UARS[5,6] (Fig. 3.2.3). Apart from the known problem areas of etalon structure, wavelength registration, and instrument degradation (see Sections 2 and 3.2.3), the results of the comparison are similar to the results of comparable exercises performed, for example, with SSBUV, SOLSPEC and SUSIM during the Atlas-1 mission[12]. It should be remembered, however, that the prime purpose of GOME is not the measurement of solar irradiance, but that the starting point for trace-gas retrievals is the I/F (earth radiance/solar flux) ratio, which is not affected by the above problems.

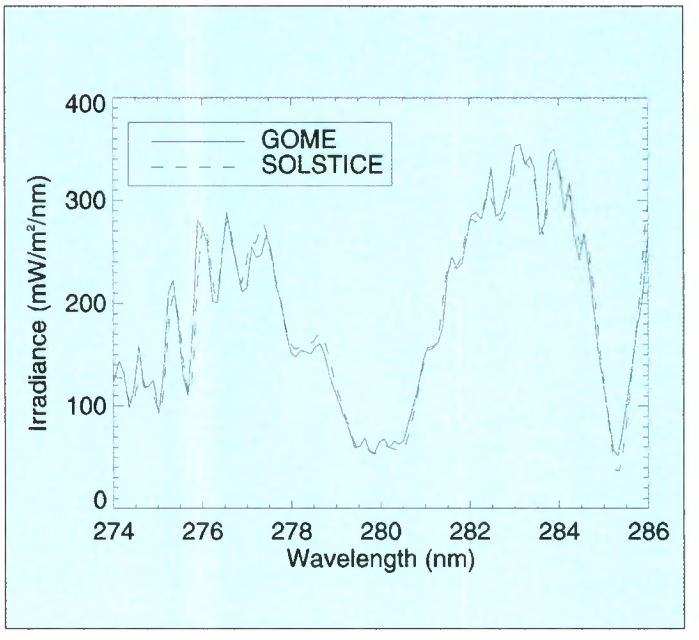

Figure 3.2.3 GOME-1 (solid line) and SOLSTICE (broken line) solar fluxes measured on 28 June 1996. Both irradiances are normalised to 1 astronomical unit. (Courtesy of P. Peeters, BISA)

3.2.3 Problem areas and remedies

Although already quite good, the wavelength determination accuracy can be improved by:

- revisiting the set of lamp lines presently used
- changing the degree of the polynom for the interpolation (and, at the channel extremes, extrapolation) for the detector regions not illuminated by lamp lines
- in the long term, introducing a wavelength calibration by using Fraunhofer lines.

The instrument degradation can be properly removed only by reprocessing the data. If, however, the rate of change is accurately characterised by a long time series, this could be extrapolated in first order, and regularly monitored to establish whether the prediction is sufficiently accurate. More work is needed in this area before a definitive solution can be implemented.

A similar rationale holds for the etalon structure, modulating the degradation curve. Potentially, this could also be removed to a large degree; but again the necessary tools are still in their infancy.

3.3 Level 2 Product: Total Ozone Column Amount (TOCA)

3.3.1 Processing steps

The level 1 to 2 processor consists mainly of four modules, plus their supporting data bases:

- The Initial Cloud Fitting Algorithm (ICFA):
  This module determines the fractional cloud within the GOME Field of View (FOV) by fitting the depth of the oxygen A-line to the measured spectrum. The cloud top height is taken from an ISCCP data base.

- The Differential Absorption Spectroscopy (DOAS) fitting:
  This involves a least-squares fitting of absorption cross-section reference spectra of O_3 (and other trace gases) to the pattern of the measured spectral radiances. As a first step, the spectral radiance is divided by the spectral irradiance. This makes the technique inherently insensitive to long-term instrument changes. In addition, the wavelength scale of the I/F ratio is scaled to the wavelength grid of the absorption cross-section reference spectrum by the 'shift and squeeze' parameters, which linearly shift (by a fixed offset) and 'squeeze' (or stretch) by another linear parameter in order that the two (I/F ratio and cross sections) match optimally. An

important adjustment parameter is the reference temperature for which the (O3) spectra are fitted.

- The Air Mass Factor (AMF) module:
  This translates the (measured) slant column into a vertical column, and comprises (in tabulated form) all the radiative-transfer computations. The basis for these AMF computations is the radiative transfer model GOMETRAN, which is based upon an MPI climatology and is modular in the constituents it considers, taking into account both multiple scattering and spherical geometry.

- The Vertical Column Determination (VCD):
  This combines the results of the previous three modules by applying to the slant columns an AMF which is determined from the fractional cloud and the complementary clear-sky air mass factors.

The final results of the processor are (geo-located) vertical columns of ozone and of NO_2. Other substances could also be retrieved in the same steps, provided:

- reference spectra of the substance are available
- air mass factors, based upon climatologies of the substance are available
- an increased computing time (or power) is available.

3.3.2 Validation status

The validation of ozone total columns seems much easier than that of radiances: there are numerous (nearly) global networks in place, and satellite data from TOMS are also available.

At mid-latitudes, the GOME TOCA results compare very favourably with ground-based measurements[13-17]. However, when going to more extreme conditions of solar zenith angle or climatological conditions, the situation changes somewhat in that there is still a significant latitude and solar-zenith-angle dependence visible[14]. In particular, processing GOME data properly emulated to the TOMS measurements, with the TOMS version 7 algorithm, reveals quite significant differences[24].

This experience is in line with the one of ground-based instruments. In an inter-comparison campaign covering various ground-based ozone instruments, the measured radiances agreed quite favourably within a few percent[33], but the largest discrepancy, of up to 40%, originated from the processing and its varying inherent assumptions and simplifications, and from the use of different ozone (and other species) absorption cross-section reference spectra.

3.3.3 Problem areas and remedies

A minor problem - but one with a serious impact on the final result - has been the use of a simplified (i.e. not based upon actual measurements) slit function to convolve the high-resolution oxygen spectra to the GOME instrument resolution. This has resulted in a systematic overestimation of the fractional cloud cover, with subsequent errors in the vertical column. This error can easily be corrected by applying the proper slit function.

Another major source of discrepancy, both with the TOMS-algorithm-processed GOME data and with the ground-based networks, is the use of the MPI climatology. Partly because of being undocumented and partly because of inherent discrepancies

and missing inputs for certain scenarios, its use has led to significantly differing results. This problem could be avoided, in principle, by using the TOMS climatology, the practical problem being that this change requires significant modifications to the GDP structure. So, although this remedy is being pursued, it will be quite some time before it can be implemented, tested and validated, and becomes operational.

3.4 Higher Level Products

From the discrete orbital tracks of the level-2 ozone data, the German Aerospace Research Institute (DLR) generates daily global maps of total ozone columns with a resolution of 1x1.25 degree, using an improved harmonic analysis technique[19].

The circulation in the lower and middle atmosphere is dominated by planetary-scale waves. Zonal sinusoidal functions, or so-called 'harmonics', are therefore well suited to describing the zonal structure of such waves, at least within narrow latitude intervals. To do so, the GOME footprint pattern of total column ozone for one day is binned into latitudinal segments of 1 degree width. The application of this technique not only permits daily ozone maps to be generated in various projections, but also allows analyses of global distribution patterns driven by wave activities in the stratosphere[20]. Figure 3.4.1 shows an example of such analyses and the underlying temporal evolution of ozone distribution.

Figure 3.4.1 Upper panel: Temporal evolution of the total column ozone zonal wave 1 amplitude from 12 to 21 September 1996 in the Southern Hemisphere. Lower Panel: South Polar stereographic projection of the total column distribution on 12 (left), 17 (centre) and 21 (right) September. (Courtesy of M. Bittner, DLR)

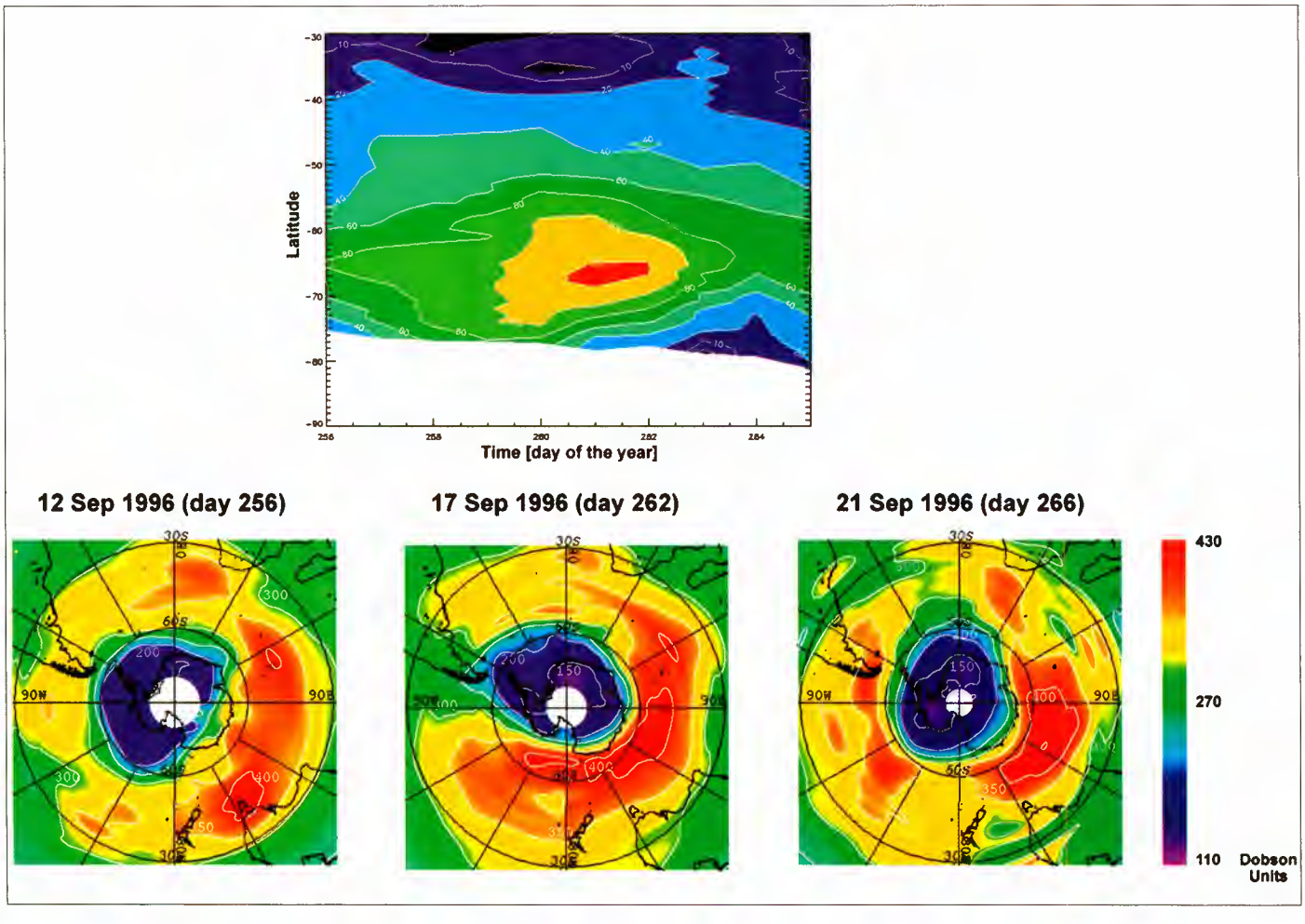

The DLR level-3 product can be accessed via:

FTP: ftp://ftp.dfd.dlr.de/atmos/gome/
ISIS: telnet:dlrpid@isis.dfd.dlr.de
WWW: http://www.dfd.dlr.de/services/

Contact/Ordering:

DFD Help Desk, Oberpfaffenhofen, Germany
Tel: +49 (0) 8153 28 2802
Fax: +49 (0) 8153 28 1343

Another approach to the generation of daily global ozone maps is pursued by the Royal Netherlands Meteorological Institute (KNMI), by ingesting the measured ozone level-2 data into an advection model using horizontal wind fields from the European Centre for Medium-range Weather Forecast (ECMWF). This product can be accessed via:

http://www.knmi.nl/onderzk/atmosam/GOME/images.html

Both the DLR and KNMI products are generated on the initiative and under the responsibility of those institutions.

3.5 Open Issues

Because of the particular situation of the ERS-2 ground segment (three distributed ground stations for the reception of X-band data) and the programmatic limitations for the inclusion of the GOME ground segment into the overall ERS-2 ground segment (no fast-delivery processors permanently installed in the ground stations; raw data copied on Exabyte cassettes and mailed to the processing centre), there is a significant time delay between data acquisition and the availability of the processed products. However, this is a financial problem rather than a technical one. In the context of a limited effort to support the CHORUS campaign, a processor was temporarily installed at the Kiruna station (covering 10 of the 14 orbits daily) and remotely operated by DLR. This processor demonstrated that a fast-delivery service (approx. 2 hours from acquisition) is possible without loss of quality for the total ozone data product[21]. Whether this temporary installation will be extended to a permanent service, at least for Kiruna but perhaps also for the other stations, is presently the subject of political discussions. The outcome will depend to a large degree on the level of funding available for the extension of the ERS-2 operational phase.

With all of the evolution in the level 0 to 1 and 1 to 2 processors, both in the past and still under implementation, there will be a need for a systematic reprocessing of the complete dataset in the near future. The timing of the start of this exercise will be determined by the availability of an updated level 1 to 2 processor with the TOMS climatology, and is realistically expected to occur only at the end of 1997. However, this does not preclude further evolution, and consequently the need for further reprocessing, in the future.

4. GOME-1 Scientific Results

4.1 Results from Radiance/Irradiance Data

4.1.1 Spectral reflectivity/albedo

A direct application of the level-1 data product is to generate the spectrally resolved surface reflectivity (and, assuming an isotropic angular behaviour, albedo)[22,23]. These data can be used for the study of surface-type spectral responses and their seasonal variability. Such potentially valuable products as vegetation indices, ocean-colour indices, short-wave top-of-atmosphere outgoing-radiation budgets, etc. can also be derived from them.

4.1.2 Mg II solar index

The Mg II core-to-wing ratio has become one of the most valuable qualitative indices of solar activity, used by both astrophysicists and geophysicists. Solar irradiance has been measured by various space-borne experiments since 1987. Instruments that have contributed data include the Solar Backscatter Ultra Violet (SBUV) experiments aboard Nimbus 7 and NOAA satellites, and two instruments on the Upper Atmosphere Research Satellite (UARS), namely SUSIM and SOLSTICE, both specifically designed for solar observations.

The MG II doublet near 280 nm is a broadband absorption feature with narrow emission peaks in the core. The h and k emission doublet originates in the Sun's chromosphere overlying the denser photosphere. The index is an indicator of solar variability on both solar 27 day rotational and solar-cycle time scales. The modulation is greater at the centre of strong lines, corresponding to radiation that originates at higher levels in the solar atmosphere. Radiation in the line wings originates in the photosphere and shows much less variability. The ratio can therefore provide an empirical representation of long-term UV solar variability. The major advantage of this core-to-wing ratio is its insensitivity to instrument artefacts. However, each instrument has its own scaling of the Mg II index, due to the spectral resolution. GOME has a higher spectral resolution than SBUV and is therefore capable of sensing solar variations more precisely.

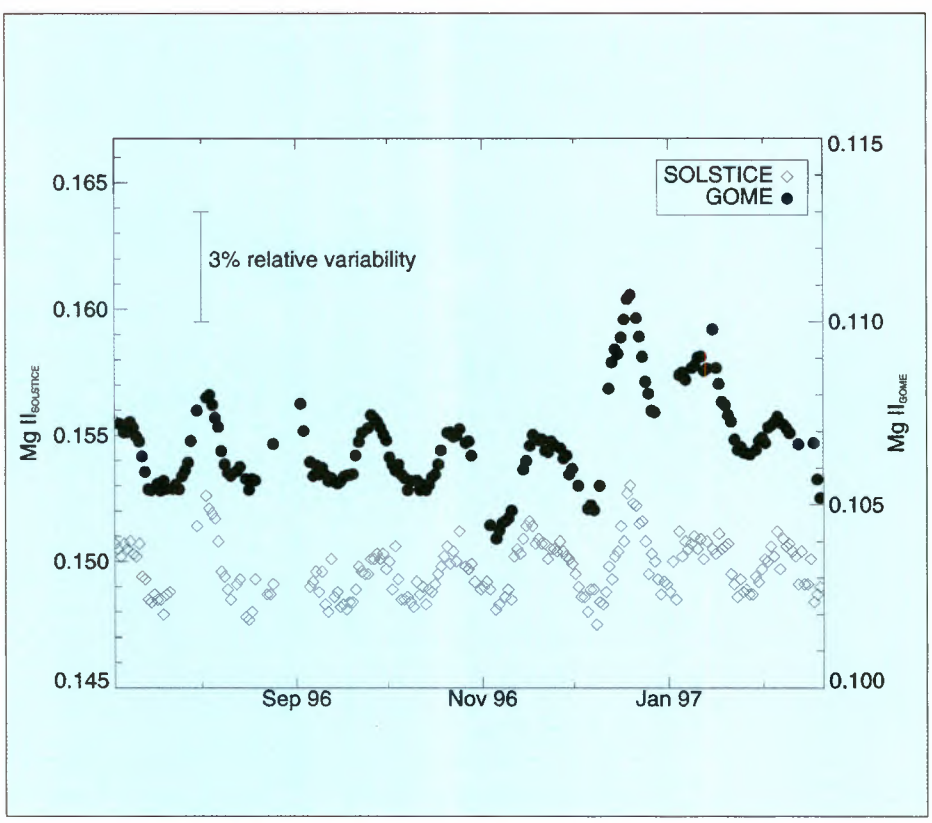

Figure 4.1.1 MG II index computed from GOME-1 solar measurements using high-resolution approach (filled circles) and corresponding SOLSTICE Mg II index (diamonds) (Courtesy of P. Peeters, BISA)

The GOME instrument makes daily solar observations during a 42 second interval when the satellite is close to the Earth's north pole. The Mg II absorption is seen in channel 1 and the emission doublet, although not fully revolved, can be clearly identified at the GOME resolution. The day-to-day precision of GOME solar measurements is better than 0.5% (2 sigma). For the analysis of the GOME Mg II index, the SOLSTICE approach has been adopted for GOME by Philippe Peeters and Paul Simon of the Belgian Institute for Space Aeronomy[6]. Since the chromospheric

emissions are resolved, integration of the peak measures the chromospheric radiation alone. The MG II index is defined as the integral of the area beneath the h and k peaks, divided by a reference intensity from the wings near the broad absorption band. The GOME Mg II index is calculated daily from an average of 150 individual GOME Sun observations. The SOLSTICE daily Mg II index is an average of the 16 individual SOLSTICE solar measurements. The comparison of both time series is plotted in Figure 4.1.1 for the period 28. June 1996 to 5 December 1996 and contains 138 individual measurements.

The very low noise of the GOME Mg II index is one of the most striking features of this plot. The 27-day rotational modulation shows up clearly on this short time series of 6 months duration. This time frame shows solar viability during the period of minimum activity between solar cycles 22 and 23.

4.1.3 Lunar albedo

Although restricted by a number of (mainly geometrical) factors, the GOME Moon calibrations can still be used, if properly processed, to derive the lunar albedo[7]. At least in the published literature, this is the first extraterrestrially measured lunar albedo for this spectral range and resolution. Figure 4.1.2 shows the result of three measurements performed in July 1995, November 1995 and September 1996, and their comparison with literature data.

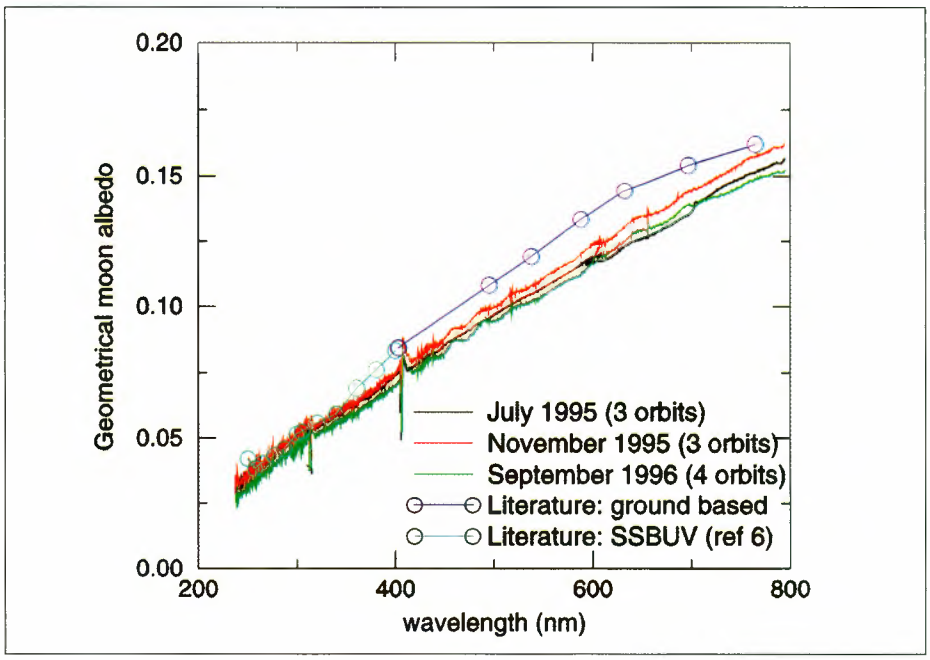

Figure 4.1.2 Averaged geometrical Moon albedos measured by GOME-1 from July 1995 (black line), November 1995 (red line) and September 1996 (green line). Ground-based literature data (blue circles) for 400 to 800 nm and SSBUV data (light blue circles) for 250 to 400 nm are also shown.
(Courtesy of M. Dobber, SRON)

4.1.4 Red-green-blue index maps

From the weighted readings of the three polarisation detectors (done at a much higher spatial resolution of 20 km x 40 km, compared to the array detectors), colour image

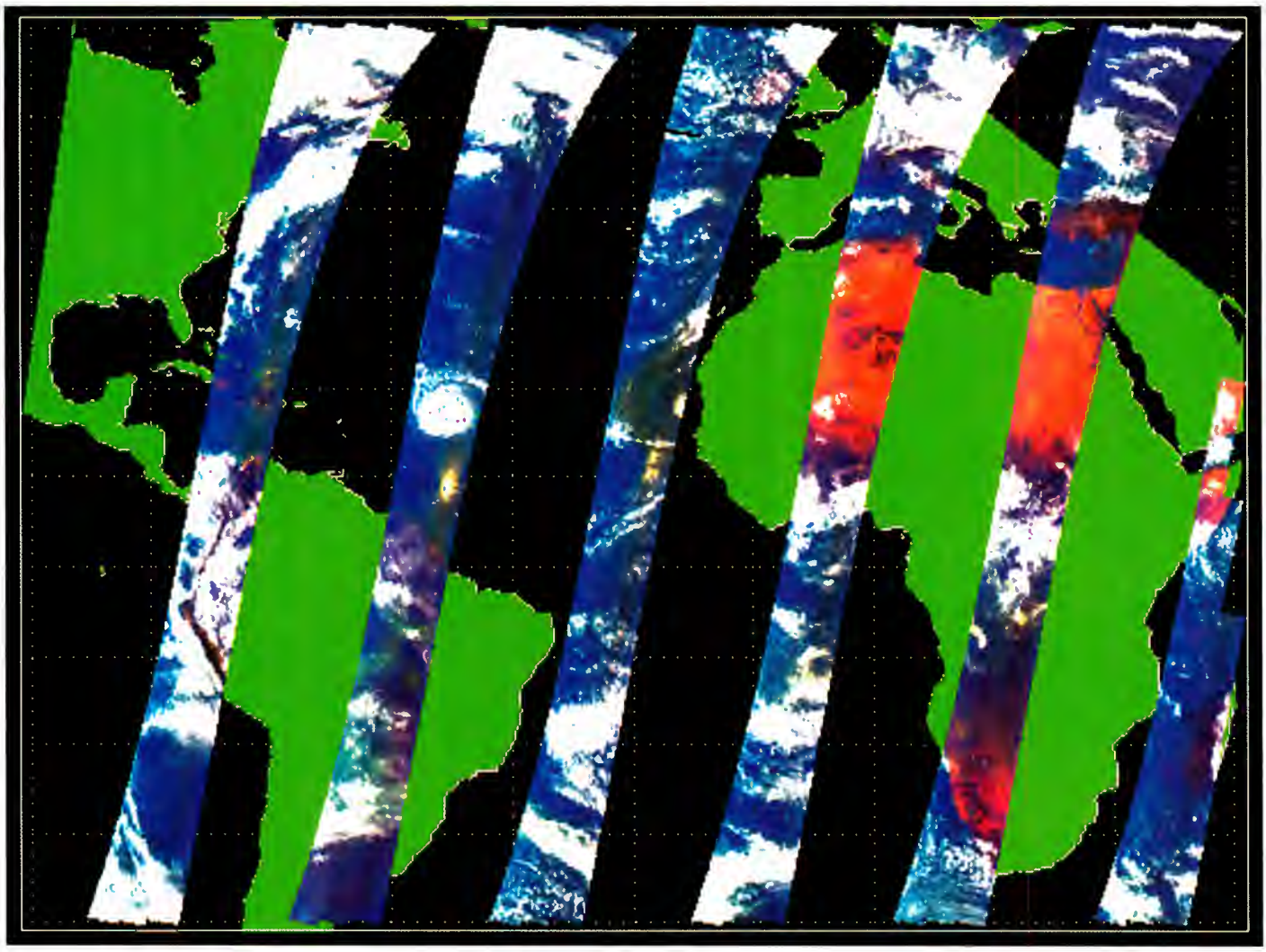

Figure 4.1.3 Colour composite of GOME-PMD measurements, acquired on 23 July 1995. The PMD images are useful for cloud detection and surface type recognition. Ground pixel size 20 x 40 km²
(Courtesy of R. Koelemeijer, KNMI)

maps can be generated[11]. These maps are not only useful, for example, to identify clear or cloudy scenes and areas of Sun glint, but can also be used for global 'quick and dirty' studies of short-wave reflectivity, cloud cover, vegetation changes, etc. (there will be probably more focused data sets for these purposes, but the direct access within the GOME scientific investigation means that these complementary data are readily available on the same time and space grid and are therefore very convenient to use!).

Figure 4.1.3 shows an example of such a map, from which such features as cloud fields, Sun-glint areas (yellowish), and desert areas can be readily identified.

4.2 Ozone Profile Retrieval

4.2.1 Retrieval approaches

Several approaches are applied to GOME data for the retrieval of ozone profiles:

SBUV: Early in the commissioning phase, the SBUV algorithm was applied to GOME data emulating the SBUV wavelengths and bandpass[24]. The algorithm converged to deliver sensible results, but no further work in this direction has been performed since.

FURM: This 'Full Retrieval Model' of the IFE Bremen is based upon either an optimal estimation retrieval technique or an Eigenvector method, both using the GOMETRAN model for the radiative transfer computations. In addition to the ozone profile proper, it also retrieves such parameters as temperature profile, Raleigh scattering parameters, surface albedo, aerosol parameters, NO_2 total amount, and Ring effect amplitude[34].

RAL Optimal Estimation: The Rutherford Appleton Laboratory (RAL) retrieval scheme also uses Optimal Estimation, with a SAGE climatology as a priori information, and GOMETRAN for the radiative transfer. The retrieval is sequentially performed on channel-1 data, yielding the upper-stratospheric profile, and then channel 2 to obtain the profile of the lower stratosphere down to ground level[26].

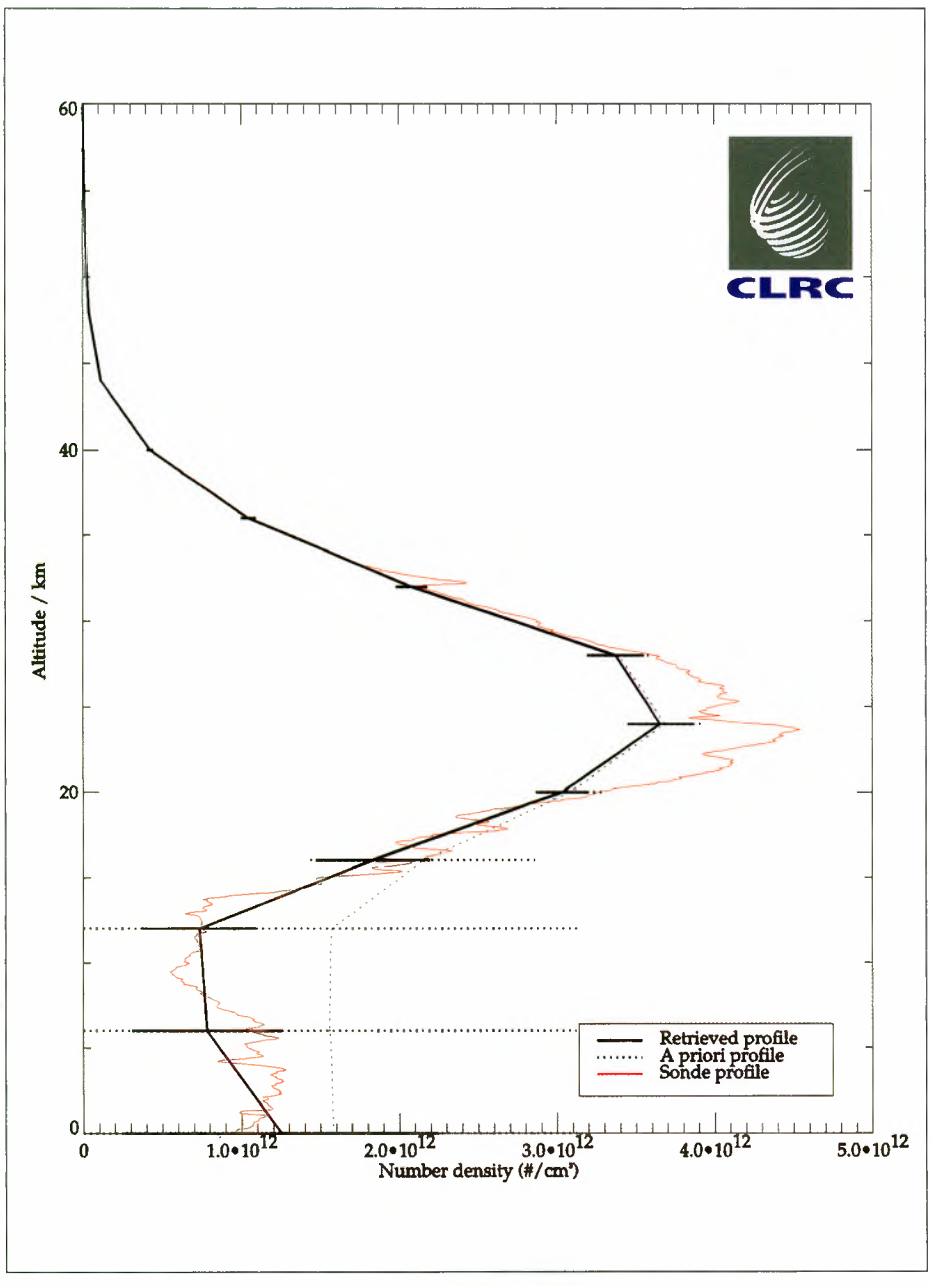

Figure 4.2.1 Retrieved GOME-1 profile (black line) from 25 July 1995 using Channel 1 and Channel 2 data for an overflight of De Bilt (NL) and corresponding sonde profile (red line). A-priori profile (dotted line) is given for information (Courtesy of R. Siddans, RAL)

SAO/DLR Approach: The two previous retrieval methods suffer from excessive computational power requirements when retrieving comprehensive and accurate profiles. SAO and DLR are cooperating in an attempt to reduce these needs, in order to devise an algorithm that is both accurate and comprehensive, and at the same time compatible with the installed computing power for an operational processor. Some initial ideas on how to reduce computing power demands have been put forward, but actual progress on this front is presently hampered by higher priority work for the SCIAMACHY instrument for Envisat.

4.2.2 Results and validation status

The RAL work provides ozone profiles from altitudes above 30 km down to ground level. The vertical resolution in the stratosphere is 4 km, while the tropospheric resolution is 6 km. Tropospheric sensitivity is such that locally enhanced pollution levels, e.g. over Southern California, could be detected.

The retrieved profiles agree very well both with satellite data obtained from MLS[27] and with ozone sonde data[26,27] (Fig. 4.2.1). Naturally, comparison of integrated profiles with the operational total ozone columns shows a strong correlation with cloud cover (not yet considered in the profile retrieval).

The FURM retrieval of IFE Bremen

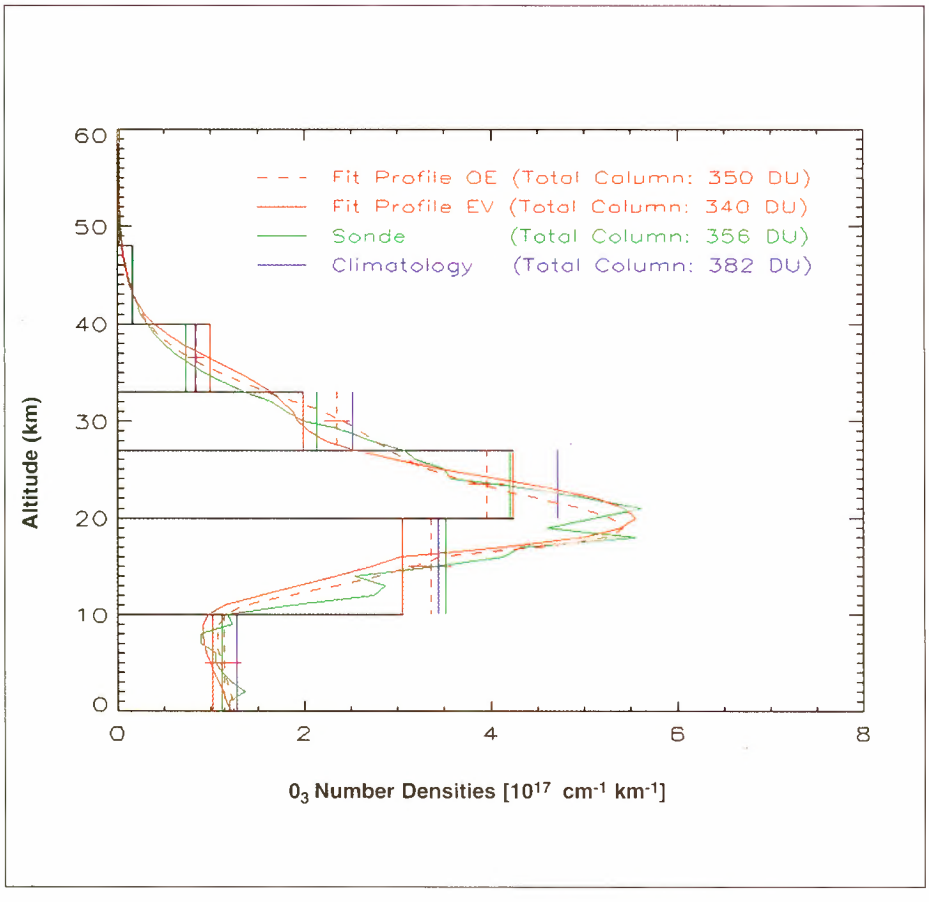

Figure 4.2.2 GOME-1 ozone profile from 4 April 1996 (52.7°N, 2.4°E) versus sonde profile (De Bilt, NL). Dashed red line: fit using a Channel 1A spectrum (289 - 307 nm) with the optimal estimation method. Solid red line: multi-window fit (289 - 307 nm and 320 - 340 nm) using the Eigenvector method. Sonde profile is given in green and climatology in blue (Courtesy of R. De Beek, IFE)

has been applied semi-operationally to GOME data in the CHORUS campaign. In order to achieve the necessary throughput, the vertical resolution and number of retrieved parameters had to be reduced. Still, the profile obtained with this scheme compares quite favourably with that from a co-located sonde launch[21] (cf. Fig. 4.2.2).

4.3 Clouds and Aerosol

4.3.1 Clouds

The retrieval of fractional cloud within the GOME ground scenes is part of the operational ozone total column processor, using climatological data for the cloud-top height. Although this works in principle quite satisfactorily, the accuracy achieved so far has been degraded by the wrong slit function being used for the convolution of the O_2 high-resolution templates. By applying the proper slit function, the accuracy will be significantly improved.

Preliminary results[23] indicate that more cloud parameters can be retrieved from the wealth of information contained in the GOME data. It is expected that, in addition to the cloud fraction, at least the cloud-top height and the average cloud optical thickness can be derived.

4.3.2 Aerosol

As the most simple approach, the TOMS algorithm for the detection of biomass burning[28], relying on the reflectivity difference between 340 and 280 nm, has been applied successfully to the GOME data, and gave meaningful geophysical results[24]. A more sophisticated algorithm, aiming at an operational cloud/aerosol processor, is starting to produce initial results for aerosol optical thickness and classification[25]. So far, these results are limited to the open ocean. With better cloud recognition and a global surface albedo database, however, it is believed that at least elevated levels of aerosol above land surfaces will also be retrievable eventually.

4.4 Minor Species

4.4.1 NO_2

NO_2 is already routinely retrieved by the GPD and reported, next to the ozone total column, in the level-2 product. Validations with ground-based DOAS instruments have shown good agreement[16]. Figure 4.4.1 shows a global NO_2 map assembled with these data.

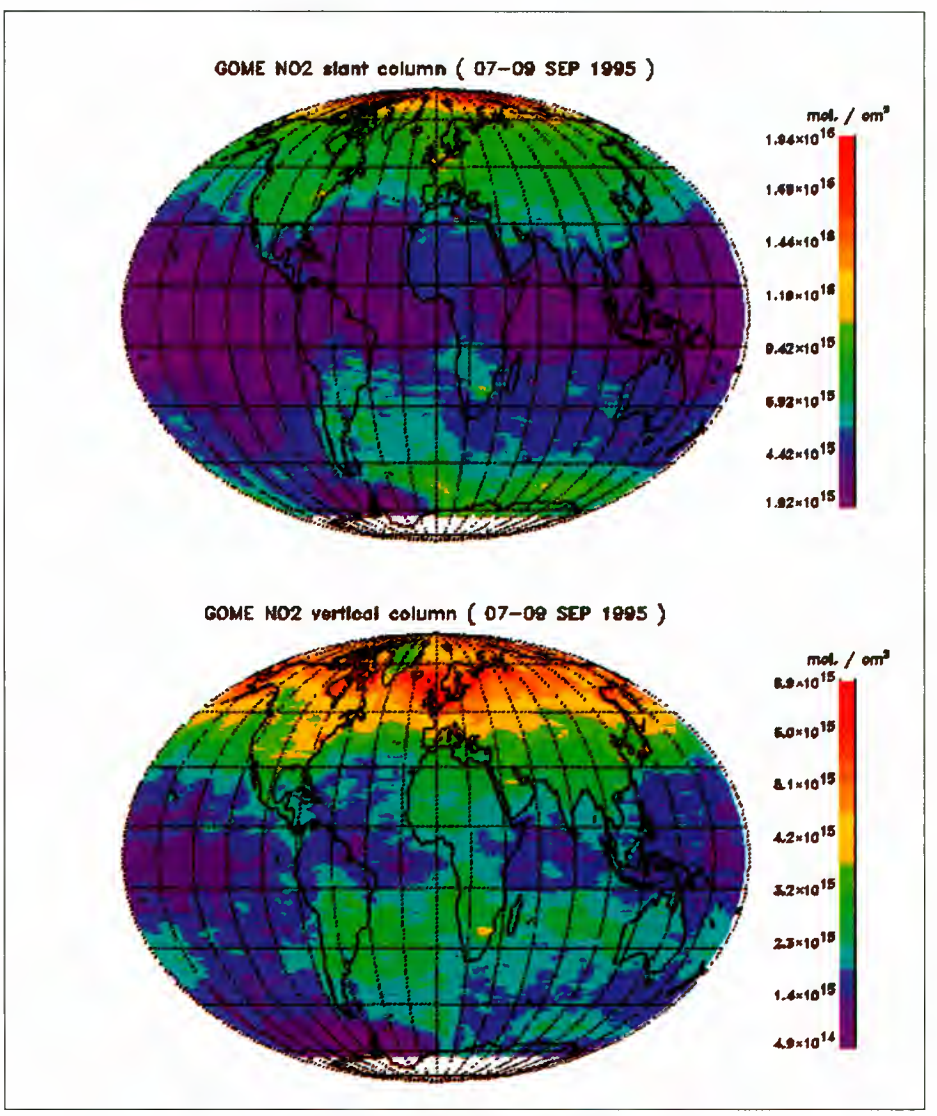

Figure 4.4.1 Level-3 projection (generated at University of Bremen by using the GOME-1 level-2 products from D-PAF) of the slant column amount of NO_2 (upper plot) and the vertical column amount of NO_2 (lower plot) for the period 7 - 9 September 1995. Plumes of high NO_2 over industrial areas such as Europe and the Eastern seaboard of the United States, Japan, Southern China, as well as the cities and biomass burning areas in Africa and South America, can be clearly seen in the lower plot (Courtesy of IFE Bremen)

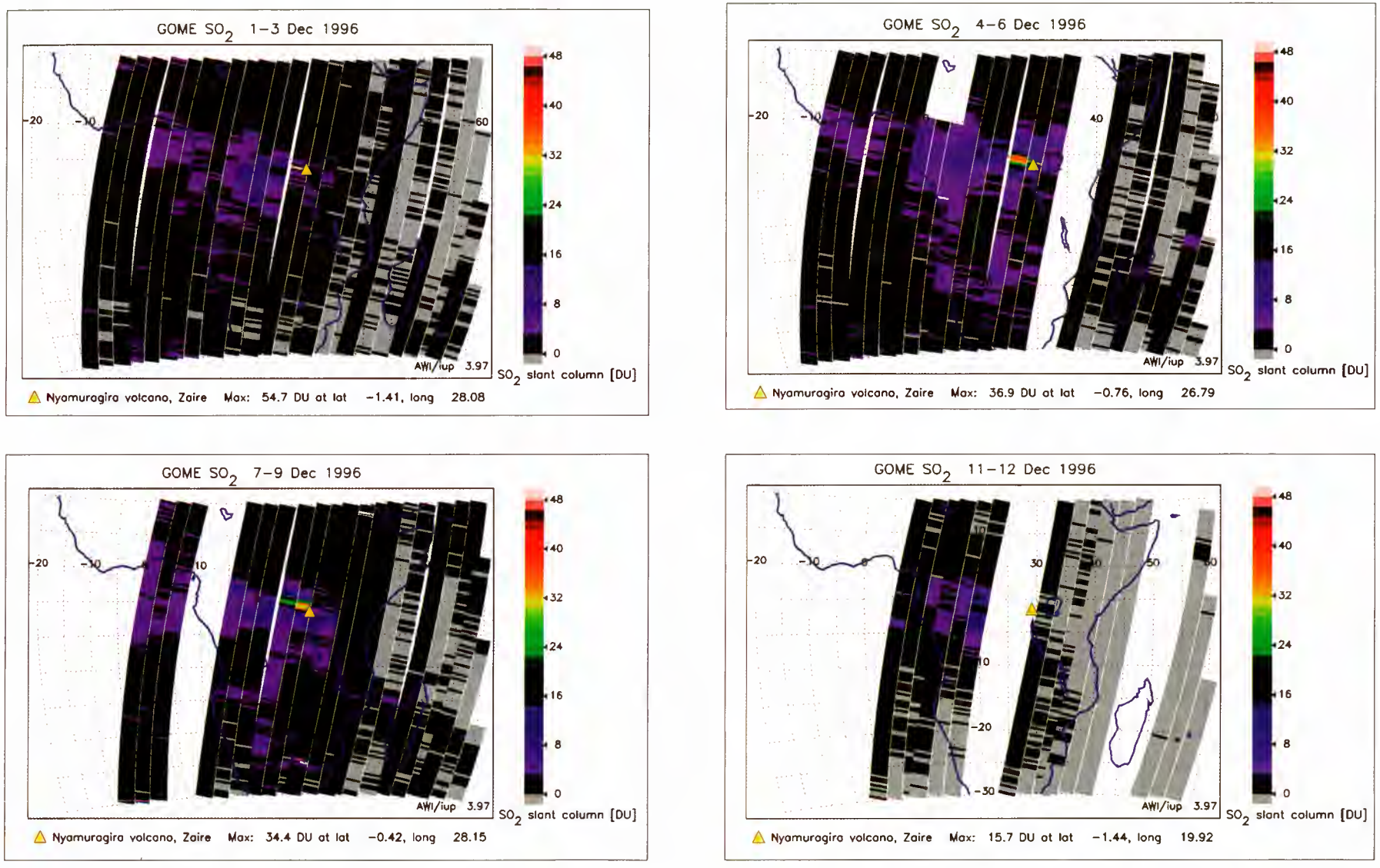

Figure 4.4.2 Three-day composites of preliminary SO_2 slant columns as measured by GOME-1 during December 1996 eruption of Nyamuragira volcano, Zaire. Only the forward-scan ground pixels are shown. Discontinuities between adjacent orbits stem from the day-to-day variability of the SO_2 plume (Courtesy of M. Eisinger, AWI)

4.4.2 SO_2

Under normal circumstances, the spectral signature of SO_2 will be masked by the ozone signature being about a factor of 100 or more stronger. With elevated SO_2 levels, however, as produced for example by particular pollution events or volcanic eruptions, it can be detected. This has been proved by the case of Nyamuragira volcano's eruption on 1 December 1996, with the plume of this eruption being traceable for several thousand kilometres and over several days (see front cover of this publication and Fig. 4.4.2)[29].

4.4.3 OClO

Being believed to be the major cause of ozone depletion during late winter and early spring, this substance plays an important role in the ozone-hole chemistry. Like SO_2, its spectral signature is normally masked by ozone, and hence its detection is limited to episodes of high OClO and low ozone, as they occur under ozone-hole conditions. Quantitative (slant) columns have been derived during the evolution of the 1996 Antarctic ozone hole's evolution, and compared to ground-based measurements, confirming the right order of magnitude for the observations[29-31]. Figure 4.4.3 shows the evolution of OClO levels for the period 23 July to 13 December 1995.

4.4.4 BrO

Because of its catalytic efficiency, BrO is believed to play a similarly important role as chlorine compounds, both in the stratosphere and in the troposphere. Being much less variable than, for example, OClO and SO_2, BrO is measurable globally. However, with an average abundance of 10-25 pptv, BrO is at the detection limit even for GOME. Nevertheless, quantitative measurements have been obtained and agree in order-of-magnitude terms with ground-based measurements[29-31].

Figure 4.4.4 shows the result of the fitting of SO_2, OClO, and BrO to the measured GOME spectra for some selected ground scenes.

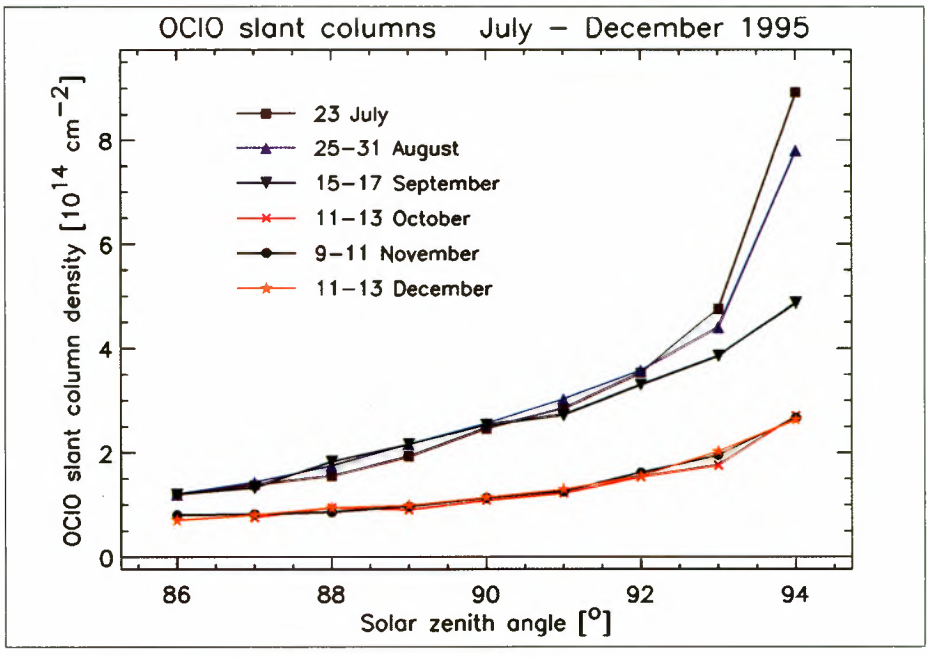

Figure 4.4.3 Antarctic OClO diurnal profiles from July to December 1995. Measurements are averaged into SZA bins. The October to December column densities have to be regarded as upper limits (Courtesy of M. Eisinger, AWI)

4.4.5 HCHO

The spectral signature of HCHO is also at the detection limit for GOME. Nevertheless, researchers at the Max-Planck Institute for Chemistry in Mainz (D) have succeeded in obtaining formaldehyde data for several sample orbits, and in correlating observed variations with known geophysical events[32].

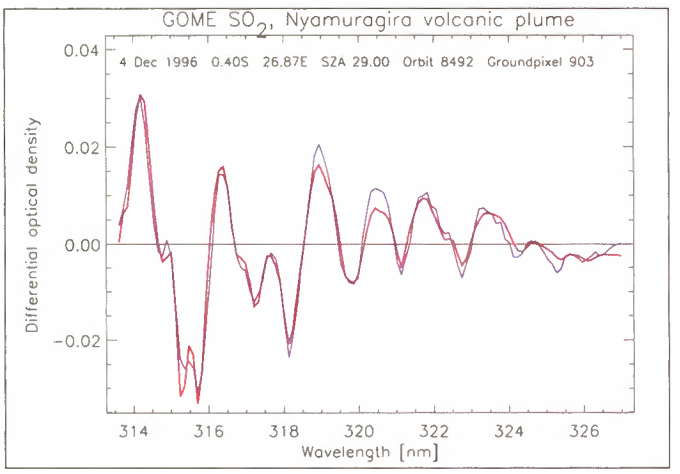

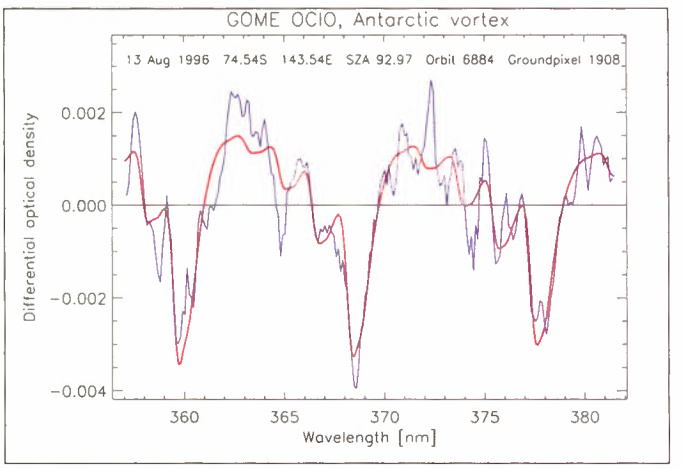

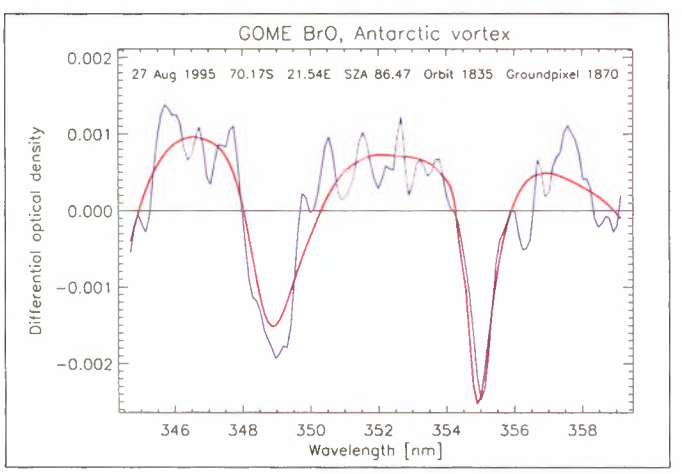

Figure 4.4.4. GOME-1 fit results (blue lines) for SO_2, OClO and BrO compared to reference absorption cross-sections measured in the laboratory (red lines). The difference between each fit result and the corresponding reference spectrum is the overall fit residual. Each spectrum represents a single selected ground pixel (Courtesy of M. Eisinger, AWI)

5. GOME-2 Expected Performances

5.1 Radiance/Irradiance

The only significant change for the level-1 radiance/irradiance products is that the presence of the white-light source is expected to remove the etalon features both in the calibration key data and in the measurement itself. With this improvement, the accuracy of the products is limited only by the accuracy of the radiometric standards used for the ground calibration. As for GOME-1, at least two independent standards will be used, and NASA will also be invited to repeat the cross-calibration with the NASA integrating sphere used for the radiometric calibration of the SSBUV/SBUV-2/ TOMS instruments. The precision of the measurements, as indicated by the Mg II index (cf. Fig. 4.1.1), is already exceptionally high.

5.2 Total Ozone

With the modifications to the scan range, optical throughput, and integration times, there are two options that can be selected for the operational scenario:

Option 1: swath 960 km, resolution 40 km x 40 km (default)
Option 2: swath 1920 km, resolution 80 km x 40 km.

Because certain inherent features of the radiative-transfer computation (e.g. Lambertian properties of surface and cloud reflectance) deviate increasingly from the real situation at more extreme viewing angles, the accuracy of the retrieved ozone column and profiles for the larger swath is believed to degrade rapidly towards the edges. To quantify these errors and set a threshold requires detailed scientific investigation.

For the default swath, with the modifications envisaged for the GOME-1 Processor (TOMS climatology and use of correct slit function for fractional cloud determination), the accuracy will be in the order of 1% and limited by features of the processor (e.g. gridding for radiative transfer/air mass factors, accuracy of ozone absorption cross-section spectra, accuracy of reference temperature for selection of cross-section spectrum, quality of Ring spectrum, etc.) rather than by instrument features. This is very much in line with the experiences of the ground-based ozone observation community[33], finding discrepancies of 10% in ozone and 30% in NO_2 for co-located measurements mainly caused by the processing and the databases used in it.

With the DOAS retrieval being very robust against any instrument changes, the long-term stability of the retrieved ozone columns is expected to be significantly better than 1% per year. The precision can be estimated from the precision of the solar-irradiance measurements and should be better than 10^{-3}.

Scene localisation accuracy depends not only on the instrument, but also to a large degree on the platform and the ground segment supporting it. Instrumental contributions to the localisation error are expected to be less than 1.5 km along-/ across-track, based upon GOME-1 experience.

5.3 Ozone Profiles

Even more than for the ozone total column, for the profiles one has to distinguish between the measurement capabilities of the instrument and the retrieval capabilities

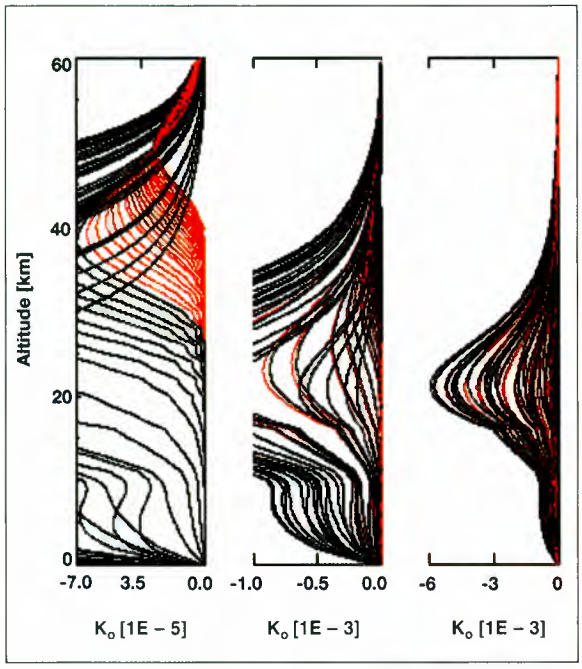

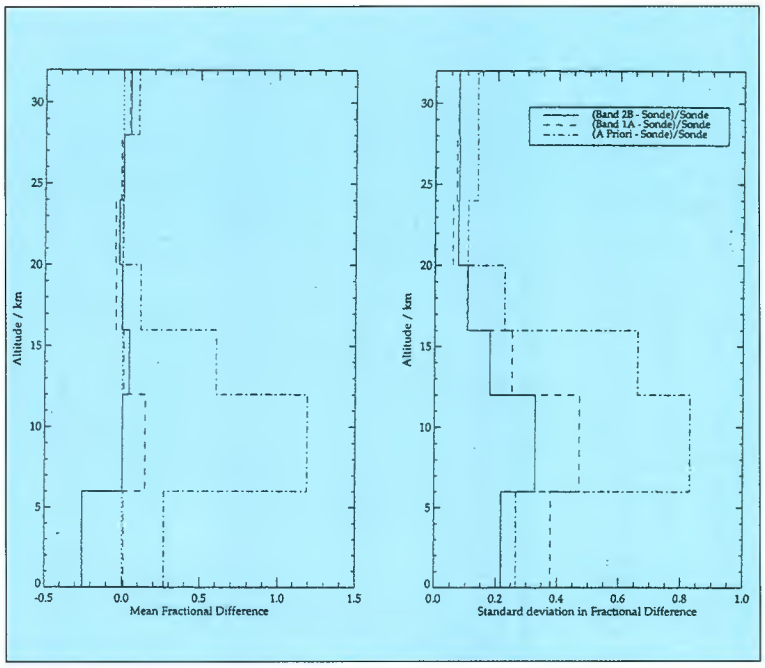

Figure 5.3.1. Ozone weighting functions calculated by GOMETRAN for a mid-latitude summer ozone profile. Red colour for 260 to 285 nm (left), 289 to 307 nm (centre), and for 320 to 340 nm wavelength (right). Starting at 260 nm, where the ozone absorption is at its maximum, the penetration depth of radiation increases. For wavelengths larger than 310 nm, significant radiation starts to reach the surfaces
(Courtesy of R. de Beek, IFE)

Figure 5.3.2. Statistics of GOME-1 ozone-profile comparison with ozone sonde data. The mean and standard deviations of differences between retrieval levels are given: a priori profiles (SAGE II January climatology), Band 1A retrieved profiles and Band 2B retrieved profiles
(Courtesy of R. Siddans, RAL)

of the processor. The instrument measurements enable the retrieval of ozone profiles in two steps:

- for the upper stratosphere, from channel-1 measurements, at a spatial resolution of 320 km x 320 km for a 960km swath (this resolution requires resampling on the ground of measurements acquired at a resolution of 320 km x 40 km)
- for the lower stratosphere/troposphere, from channel-2 measurements, at a spatial resolution of 40 km x 40 km for a 960 km swath.

The vertical resolution achievable by the GOME-2 instrument is restricted by the nature of the radiative transfer in the atmosphere. Figure 5.3.1. shows the weighting functions for various wavelengths used for the profile retrieval. From these weighting functions, one can estimate that the limits for vertical resolution are 6 km in the troposphere and 4 km from 14 km to 60 km[34].

As regards the accuracy of the measurements, comparisons with ozone sonde data suggest that, even with the limited processor available today, the accuracy is generally in the order of better than 10% (Fig. 5.3.2 from Ref.[26]). For a rigorous comparison, the sonde errors also have to be taken into account.

Much more than the total column, the accuracy of the retrieved profile information will be influenced by 'auxiliary' information which can, in principle, be retrieved from the measurement itself, but at the expense of (probably prohibitive) computing power:

- fractional cloud, cloud altitude within the ground scene
- temperature profile and its accuracy
- surface albedo and its accuracy
- aerosol load
- interfering species, such as elevated levels of SO_2.

5.4 Clouds and Aerosol

5.4.1 Clouds

Whilst the fractional cloud within a ground scene is already part of the total ozone column retrieval and product, the data contain a vast amount of additional information, the exploitation of which is in its infancy. Typical key features in terms of potential cloud information include:

- radiance threshold, for both for the spectrally resolved and the polarisation channels
- 'colour' of the scene from RGB ratios
- depth of O_2 bands (although A, B, and γ band do not contain independent information with respect to the radiative transfer, they do with respect to instrument properties, like signal-to-noise ratio)
- O_2/O_4 equilibrium, indicating the pressure at the scattering level (i.e. cloud top height or surface)
- Ring-effect amplitude[18]
- polarisation.

From all of these independent parameters, it should be possible to retrieve fractional cloud to within 10% of the scene coverage, cloud top height to within better than 100 mbar, and cloud optical depth. Measurement of the degree of polarisation might further enable the detection of cirrus clouds and polar stratospheric clouds, even over bright snow/ice surfaces.

5.4.2 Aerosol

Because of the complexity of aerosol in terms of its composition (e.g. soot, sulphate, mineral, maritime), size (mean and distribution), vertical distribution (boundary layer, troposphere, stratosphere), and dependence on relative humidity, a commitment cannot be made at this stage that the full catalogue of the World Meteorological Organisation (WMO) classified aerosols will be retrievable under all circumstances. Hence, a reliable aerosol retrieval might be eventually restricted to:

- certain classes of aerosol: e.g. stratospheric volcanic, sooty, maritime
- certain observational conditions, in particular cloud-free scenes over open ocean.

As work on all of these aspects is still in its infancy, any far-reaching promises would be premature at this point.

5.5 Other Species

The measurement capabilities of the GOME-2 instrument are expected to be the same as for GOME-1 in this respect; i.e. it is expected that NO_2 and BrO can be retrieved globally, and OClO, SO_2, HCHO, and potentially others under special observational conditions (e.g. OClO under ozone-hole conditions, SO_2 at elevated levels due to pollution events or volcanic eruptions, HCHO for major biomass burning events). To what degree this 'thresholding' will be implemented in the operational processor is at present under investigation, at least for some of the species.

A particular case in which the spectral signature has been clearly seen in the spectra, but no actual retrieval has yet been performed, is that of water vapour. The main reason for this is the lack of accurate high-resolution absorption cross-section spectra for the necessary temperature range. If these were available, a total column and possibly even some profile information might be retrievable. How such a product could compete with, for example, microwave soundings of humidity cannot yet be assessed.

6. Summary and Conclusions

6.1 GOME-1 Achievements

Table 6.1.1 compares the 'expected' list of species, as established in Table 2.1 of Reference[35] long before the launch of GOME, with the list of species actually observed today (March 1997).

Species	Qualification	Status
O_3		yes, see paras. 3.3 and 4.2
NO (above 40 km)		observed, but not quantitatively retrieved
NO_2		yes, see para. 3.3
BrO		yes, see para. 4.4
H_2O		observed, but not quantitatively retrieved
O_2-O_4		O_2 used for cloud; O_4 observed but not retrieved
Aerosols		experimental retrieval, see para. 4.3
Partial Coverage or Occasional Observation		
SO_2	tropospheric pollution; volcanic events	yes, see para. 4.4
HCHO	tropospheric pollution, biomass burning	yes, see para. 4.4
OClO	twilight ozone-hole conditions	yes see para. 4.4
BrO	ozone-hole conditions	yes, see para. 4.4
ClO	ozone-hole conditions	no*
NO_3	twilight conditions, i.e. close to the terminator	no*
PSCs		no**

* The species ClO and NO_3 have not been actively looked for yet; they might eventually turn out to be retrievable also.

** In the case of PSCs, fundamental problems in detecting them against a background of ice and snow are expected.

Table 6.1.1. 'Observed' versus 'target' molecules

Table 6.1.2 summarises the main features of the operational GOME Data Processor as presently installed, and the initial key parameters of the scientific ozone profile retrieval.

Table 6.1.2. Main features of ozone data from GOME-1

Swath width (default)	960 km global coverage within 3 days, above 45° lat. daily cover
Spatial sampling	320×40 km^2 (Channels 2–4)* 960×120 km^2 (Channel 1)
Total ozone column scene size	320×40 km^2
Ozone profile upper stratospheric scene size	960×120 km^2
Ozone profile lower stratosphere/tropospheric scene size	320×40 km^2
Vertical range	0–60 km
Vertical resolution	0–12 km: 6 km** 14–60 km: 4 km**
Profile accuracy	0–12 km: <20%** 14–60 km: <10%**
Geo-location accuracy	1.5 km along-/across-track, plus satellite/system contributions

* Measurements are made at 80×40 km, co-added onboard because of telemetry restrictions.

** These parameters are strongly dependent on algorithm/processing power.

6.2 GOME-2 Expectations

Basically, the list of observable species/parameters for GOME-2 will be the same as for GOME-1. The technical modifications envisaged, in particular the much more comprehensive polarisation measurement capabilities, are expected to improve:

- the capabilities for detecting clouds and quantify cloud parameters
- the potential for aerosol classification and parameter retrieval
- the chance of detecting polar stratospheric clouds by means of their polarisation signature.

With an improved optical throughput and a much more comfortable telemetry allocation, the major difference between GOME-1 and GOME-2 lies in the spatial resolution. The expected performances for ozone total column and ozone profiles are listed in Table 6.2.1 for the default case of a 960 km swath.

Swath width (default)		960 km global coverage within 3 days daily coverage above 45° lat.
Total Ozone Column		
Spatial sampling		40×40 km^2
Accuracy		<1%
Precision		<1%
Ozone Profiles		
Upper/middle stratosphere		320×320 km^2
Lower stratosphere/troposphere		40×40 km^2
Vertical range		0–60 km
Vertical resolution	0–12 km: 14–60 km:	6 km 4 km
Accuracy	0–12 km: 14–60 km:	<10% <5%
Precision		<1%
Stability		<1%
Geo-location accuracy		1.5 km along-/across-track, plus satellite system contribution

Table 6.2.1 Main features of ozone data from GOME-2

6.3 Conclusions

With the experience of having an instrument in orbit for nearly two years, and the data being processed, scientifically evaluated, and validated, one can draw a number of important conclusions, which are also of relevance for GOME-2:

Even for an instrument performing as well as GOME-1, there is room for improvement and fine tuning. All operational instruments for METOP are at least second-generation, and some of them have gone through even more design-change loops, implementing feedback from several years of operations (HIRS4)

No instrument can claim to be absolutely free from degradation in the harsh environment of space. It is therefore necessary to account for this by devising robust, comprehensive, and redundant (not in the sense of redundant units, but redundant paths to monitor) on-board calibration systems.

However, all of these calibration tools are useless without:
- the necessary ground processing system in place to evaluate and exploit the data
- the scientific and engineering manpower needed to interpret the data, and
- the countermeasures in the processing to account for observed degradation mechanisms.

It is therefore an illusion to believe that a data-processing system can be developed and tested, and after a certain commissioning effort can be left alone for routine operations. It takes continuous monitoring, both for instrument effects and for processing artefacts, to generate reliable, high-quality long-term data sets.

The fainter an instrument degradation mechanism, the longer it takes to quantify it with good accuracy. In many cases, one will have to wait and evaluate data for a year or more before quantitative statements can be made and countermeasures put in place. If the quality of the data set is to be maintained, this implies the need for a regular reprocessing of the data. The sizing of processing capacities has to take that into account.

As much error as comes from a space instrument and its potential degradation can be introduced by the processing. The atmosphere, with its variability in space, time, composition, cloudiness, aerosol load, surface albedo, etc. is a complex system, in which by far not all parameters are well-controlled and understood. The processing is therefore based upon inherent simplifications, necessarily introducing errors. Keeping these errors at a tolerable level is a major challenge for the processing-system developer.

There is a pronounced difference between a scientific algorithm for processing data and an operational one. Whereas a scientific algorithm can strive for the ultimate accuracy - for example by applying sufficiently fine gridded radiative transfer modelling, simultaneous retrieval of all relevant parameters, numerous iterative loops until the result is satisfactory - an operational processor has to cope with the throughput requirement, i.e. the system has to process data sets at the same rate as they are acquired (and should still have margins to account for reprocessing, down times, maintenance activities, etc.). This requires trade-offs between the cost of the system and its performance. The art is then to find the right balance between investment cost and performance limitations, e.g. in terms of accuracy, resolution, number of parameters retrieved, etc.

In addition to the errors introduced by the processing, biases result from the use of input data bases necessary for the processing. Prominent examples for such biases are: the selection of absorption cross-section spectra for ozone and interfering or retrieved species; climatology underlying the radiative-transfer computation; the selection or source of the reference temperature in the atmosphere used to select the proper ozone cross-section spectra; and the origin and accuracy of the Ring spectrum.

Only by the conscious selection and proper documentation of these parameters can confusion be avoided when comparing data sets of different origins (see Ref. 33 also as an example).

Finally, the need has to be stressed for a continuous validation of the data set, by means of independent observations of all relevant parameters. Clearly, this has to account for assessing coincidence in time and space, and for the inherent errors and biases of the methods applied and the instrument itself. Only with such a concerted effort can one be confident that the final data set will be of a quality that enables valid conclusions to be drawn for the monitoring of our climate.

Acknowledgement

The work reported here is the result of a collaborative effort by many scientists in Europe and the United States, not only since the GOME instrument has been in orbit and producing data, but since the very beginning of the GOME programme back in the late 1980s. The most important support over the long term has come from the GOME lead scientist John Burrows from IFE in Bremen. He and his co-workers and students have not only put their signature on the instrument but also on the processor, and they are now actively putting the data to their ultimate scientific use.

Shortly after the approval of the instrument for ERS-2, John Burrows was joined by the members of the GOME Science Advisory Group chaired by my ESA colleague Christopher Readings: K. Chance and R. Spurr (SAO, USA), A. Goede (SRON, NL), P. Stammes (KNMI, NL), D. Perner (MPI Mainz, D), U. Platt (Univ of Heidelberg, D), J.P. Pommereau (CNRS, F), P. Simon (BISA, B), R. Guzzi (IMGA, I), B. Kerridge (DRAL, UK). The key people responsible for the processor were W. Balzer and D. Loyola (DLR, D).

They were joined by numerous scientists supporting the specialised subgroups for instrument calibration and characterisation, data processing and algorithm development, and validation. Others joined in when the GOME data became available to users selected on the basis of the 'Announcement of Opportunity for the Utilisation of ERS Data'.

The author would especially like to acknowledge the support received through the faithful collaboration of our colleagues at NASA's Goddard Space Flight Center, in particular E. Hilsenrath and J. Gleason.

Last but not least, the author would like to thank several ESA colleagues without whom we would not be where we are today: J. Callies, A. Lefèbvre and C. Caspar from ESTEC (NL), F. Bosquillon from ESOC (D), and C. Zehner, R. Koopmann and D. Pemberton from ESRIN (I).

References

1. Caspar C. & Chance K, 1997, GOME Wavelength Calibration Using Solar and Atmospheric Spectra, Proc. Third ERS Scientific Symposium, Florence, 17-21 March 1997, ESA SP-414, May 1997.

2. Hahne A., Lefèbvre A., Callies J. & Christensen B. 1995, GOME: The Development of a New Instrument, ESA Bulletin No. 83, August 1995, p. 41.

3. Hahne A. et al. 1995, The Global Ozone Monitoring Experiment (GOME) Users Manual, ESA SP-1182, September 1995.

4. Aben I. & Goede A. 1997, First Results on GOME Breadboard Measurements on Vacuum Characteristics and Atmospheric Radiation (GOBELIN Project), Proc. Third ERS Scientific Symposium, Florence, 17-21 March 1997, ESA SP-414, May 1997.

5. Peeters P., Simon P.C., Rottmann G. & Woods T.N. 1996, UARS SOLSTICE Data as a Calibration and Validation of GOME, Proc. GOME Geophysical Validation Campaign Final Results Workshop, January 1996, ESA WPP-108, April 1996, p.75.

6. Peeters P., Simon P., White O.R., De Toma G., Rottmann G.J., Woods T.N. & Knapp B.G. 1997, MgII Core-to-Wing Solar Index from High-Resolution GOME Data, Proc. Third ERS Scientific Symposium, Florence, 17-21 March 1997, ESA SP-414, May 1997.

7. Dobber M.R. 1997, GOME Mon Measurements, Including Instrument Characterisation and Moon Albedo, Proc. Third ERS Scientific Symposium, Florence, 17-21 March 1997, ESA SP-414, May 1997.

8. Pemberton D. 1997, GOME Diffuser and Dark Signal Trends, Proc. Third ERS Scientific Symposium, Florence, 17-21 March 1997, ESA SP-414, May 1997.

9. Stammes P., Koelemeijer R.B.A., Stam D.M. & Aben I.1996, Validation of GOME Polarisation and Radiance Measurements, Proc. GOME Geophysical Validation Campaign Final Results Workshop, January 1996, ESA WPP-108, April 1996, p.41.

10. Koopmann R. 1997, Analysis of GOME Straylight, Proc. Third ERS Scientific Symposium, Florence, 17-21 March 1997, ESA SP-414, May 1997.

11. Koelemeijer R.B.A, Stammes P. & Watts P. 1997, Comparison of Visible Calibrations of GOME and ATSR-2, Submitted to: Remote Sensing of Environment, February 1997.

12. Cebula R.P., Thuillier G.O., Hoosier M.E., Hilsenrath E., Herse M., Brueckner G.E. & Simon P.C. 1996, Observation of the Solar Irradiance in the 200-350nm Interval during the ATLAS-1 Mission: A Comparison among Three Sets of Measurements - SSBUV, SOLSPEC, and SUSIM., Geophys. Res. Lett. 23, No. 17, pp. 2289-2292.

13. Lambert J.C. et al. 1996, GOME Total Ozone Amount Validation by Ground Based Observations Performed at the NDSC Alpine Station, Proc. GOME Geophysical Validation Campaign Final Results Workshop, January 1996, ESA WPP-108, April 1996, p.109

14. Lambert J.C. et al. 1996, GOME Products Validation with the SAOZ Network, Proc. GOME Geophysical Validation Campaign Final Results Workshop, January 1996, ESA WPP-108, April 1996, p.123

15. Schoubs E. & De Muer D. 1996, Validation of ERS-2 GOME Ozone Data by Ground Based Observations at Uccle (Belgium), Proc. GOME Geophysical Validation Campaign Final Results Workshop, January 1996, ESA WPP-108, April 1996, p.133.

16. Tuerk A., Callies J., Lefèbvre A., Hahne A., Richter A. & Burrows J.: Observations of O_3 and NO_2 with the GOME BBM during In-orbit Validation of the ERS-2 GOME, Proc. GOME Geophysical Validation Campaign Final Results Workshop, January 1996, ESA WPP-108, April 1996, p.255.

17. Piters A. 1997, GOME Validation Using Data Assimilation, Proc. Third ERS Scientific Symposium, Florence, 17-21 March 1997, ESA SP-414, May 1997.

18. Joiner J.J. & Bhartia P.K. 1995, The Determination of Cloud Pressures from Rotational Raman Scattering in Satellite Backscatter Ultraviolet Measurements, J. Geophys. Res. 100, D11, 20.019-20.026, November 1995.

19. Bittner M., Dech S., Ruppert T., Loyola D. & Balzer W. 1996, Prospective GOME-Level 3 Products, Technical Report D82234, DLR-DFD, Oberpfaffenhofen, Germany.

20. Bittner M, Dech S. & Loyola.D. 1997, Planetary Scale Waves in Total Ozone Data from ERS-2 GOME, Proc. Third ERS Scientific Symposium, Florence, 17-21 March 1997, ESA SP-414, May 1997.

21. Eichmann K.U. 1997, Ozone Profile Retrieval from GOME Satellite Data, II: Validation and Applications, Proc. Third ERS Scientific Symposium, Florence, 17-21 March 1997, ESA SP-414, May 1997.

22. Koelemeijer R.B.A., Stammes P. & Stam D.M. 1997, Spectral Surface Albedo Derived from GOME Data, Proc. Third ERS Scientific Symposium, Florence, 17-21 March 1997, ESA SP-414, May 1997.

23. Stammes P., Stam D.M. & Koelemeijer R.B.A. 1996, Spectral Reflectivity and Polarisation of Clouds over Ocean as Measured by GOME On Board ERS-2. In: IRS=96: Current Problems in Atmospheric Radiation (Eds. W.L. Smith and K. Stamnes), Deepak Publ. (1996).

24. Gleason J., NASA Goddard Space Flight Center, Private Communication.

25. Mochi M., Bartoloni A., Serafini C., Cervino M., Levoni C. & Cattani E.1997, GOME Data Processing at I-PAF: The Aersol Optical Thickness Retrieval from GOME Spectra, Proc. Third ERS Scientific Symposium, Florence, 17-21 March 1997, ESA SP-414, May 1997.

26. Siddans R. 1997, Height-Resolved Ozone Information from GOME, Proc. Third ERS Scientific Symposium, Florence, 17-21 March 1997, ESA SP-414, May 1997.

27. Munro R., Siddans R., Reburn W.J. & Kerridge B.J. 1997, Height-Resolved Ozone Information from GOME Flight Data, Proc. XVIII Quadrennial Ozone Symposium, L'Aquila, Italy, 12-21 September 1996, WMO, in press.

28. Hsu N.C., Herman J.R., Bhartia P.K., Seftor C.J., Torres O., Thomson A.M., Gleason J.F., Eck T.F. & Holben B.N.1996, Detection of Biomass Burning Smoke from TOMS Measurements, Geophys. Res. Letters 23, No. 7, pp. 745-748.

29. Eisinger M., Burrows J.P., Richter A. & Ladstaetter-Weissenmayer A. 1997, SO2, OClO, BrO, and Other Minor Trace Gases from the Global Ozone Monitoring Experiment, Proc. Third ERS Scientific Symposium, Florence, 17-21 March 1997, ESA SP-414, May 1997.

30. Eisinger M., Burrows J.P. & Richter A. 1996, Studies on the Precision of GOME Irradiance and Radiance Products and GOME Measurements of OClO and BrO over Antactica, Proc. GOME Geophysical Validation Campaign Final Results Workshop, January 1996, ESA WPP-108, April 1996.

31. Hegels E., Crutzen P.J., Tuepfel T. & Perner D. 1997, Global Ozone Monitoring Experiment: Global Distrubtion of BrO, Proc. Third ERS Scientific Symposium, Florence, 17-21 March 1997, ESA SP-414, May 1997.

32. Perner D., Kluepfel T., Helges E., Crutzen P.J. & Burrows J.1997, First Results on Tropospheric Observations by the Global Ozone Monitoring Experiment, GOME, on ERS-2, Proc. Third ERS Scientific Symposium, Florence, 17-21 March 1997, ESA SP-414, May 1997.

33. Vanghan G.et al (24 co-authors) 1997, An Intercomparison of Ground-Based UV-Visible Sensors of Ozone and NO2, J. Geophys. Res. 102, D1, 1411-1422, January 1997.

34. De Beek R., Hoogen R., Rozanor V. & Burrows J.P. 1997, Ozone Profile Retrieval from GOME Satellite Data. I: Algorithm Description, Proc. Third ERS Scientific Symposium, Florence, 17-21 March 1997, ESA SP-414, May 1997.

35. Guyenne T.D. & Readings Ch (Eds.) 1993, Global Ozone Monitoring Experiment Interim Science Report, ESA SP-1151, September 1993.

36. Callies J., Lefèbvre A., Caspar C. & Hahne A., Stability of the Engineering Calibration Parameters of GOME on board ERS-2, Proc. XVIII Quadrennial Ozone Symposium, L'Aquila, Italy, 12-21 September 1996, WMO, in press.

Annex
List of GOME-Related Pages on Internet

The ESA-ESRIN GOME Home Page:

http://pooh.esrin.esa.it:8888/eeo/fr/eeo4.63/eeo4.96

includes general information and daily updated GOME performance results.

The site of the GOME Lead Scientist:

http://www-iup.physik.uni-bremen.de/ifepage/gome.html

includes ozone and NO_2 maps.

The site of the Ground Processing Facility:

http://www.dfd.dlr.de/info/AUC/GOME/index.html

includes data-product descriptions and products.

Near-real-time information is available at:

http://www-iup.physik.uni-bremen.de/ifepage/geomenrt.html
http://www.dfd.dlr.de/info/AUC/GOME/index.html
http://www.knmi.nl/onderzk/atmosam/GOME/images.html

European Space Agency
Agence spatiale européenne

Contact: ESA Publications Division
c/o ESTEC, PO Box 299, 2200 AG Noordwijk, The Netherlands
Tel (31) 71 565 3400 - Fax (31) 71 565 5433